Article

Transmigration of *Trypanosoma brucei* across an *in vitro* blood-cerebrospinal fluid barrier

Application of different *T.brucei brucei* strains to *in vitro* blood-CSF barrier

HIBCPP cells on transwell filter inserts simulate choroid plexus epithelium

Quantification of transmigrated parasites by qPCR

10   15   20   25   30

Annika Speidel, Marianne Theile, Lena Pfeiffer, ..., Horst Schroten, Michael Duszenko, Stefan Mogk

stefan.mogk@uni-tuebingen.de

Highlights
HIBCPP cells on Transwell filters were used as a model of the blood-CSF barrier

Transmigration efficiency of *Trypanosoma brucei brucei* was quantified by qPCR

Transmigration seemed independent of major surface metalloprotease B

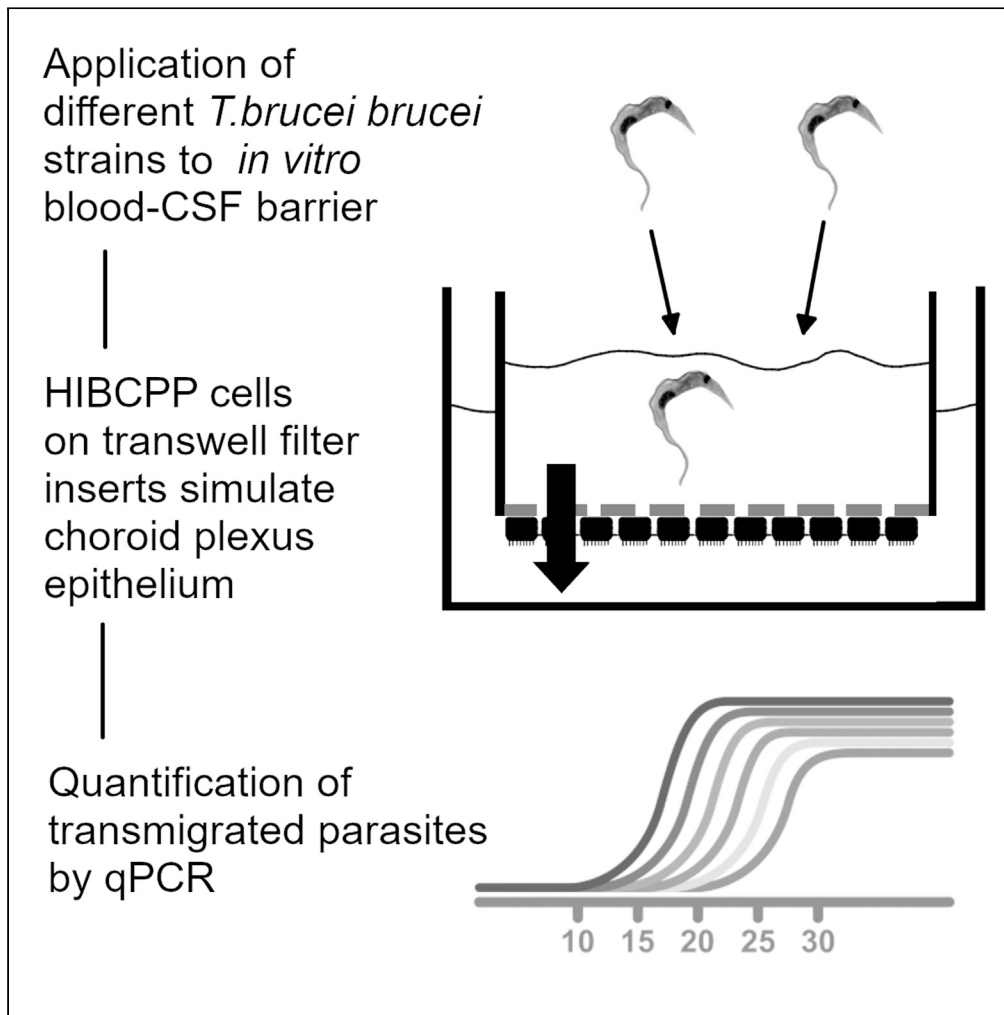Transmigration might be a mechanical process affected by parasite geometry/motility

Article

Transmigration of *Trypanosoma brucei* across an *in vitro* blood-cerebrospinal fluid barrier

Annika Speidel,[1] Marianne Theile,[1] Lena Pfeiffer,[1] Alexander Herrmann,[1] Katherine Figarella,[2] Hiroshi Ishikawa,[3] Christian Schwerk,[4] Horst Schroten,[4] Michael Duszenko,[2] and Stefan Mogk[1,5,*]

SUMMARY

***Trypanosoma brucei* is the causative agent of human African trypanosomiasis. The parasite transmigrates from blood vessels across the choroid plexus epithelium to enter the central nervous system, a process that leads to the manifestation of second stage sleeping sickness. Using an *in vitro* model of the blood-cerebrospinal fluid barrier, we investigated the mechanism of the transmigration process. For this, a monolayer of human choroid plexus papilloma cells was cultivated on a permeable membrane that mimics the basal lamina underlying the choroid plexus epithelial cells. Plexus cells polarize and interconnect forming tight junctions. Deploying different *T. brucei brucei* strains, we observed that geometry and motility are important for tissue invasion. Using fluorescent microscopy, the parasite's moving was visualized between plexus epithelial cells. The presented model provides a simple tool to screen trypanosome libraries for their ability to infect cerebrospinal fluid or to test the impact of chemical substances on transmigration.**

INTRODUCTION

Human African trypanosomiasis (HAT) or sleeping sickness is an infectious disease caused by the unicellular eukaryotic flagellated parasite *Trypanosoma brucei* (Brun et al., 2010) that lives in blood, lymphatic system, and interstitial spaces of organs (Kennedy, 2013). These trypanosomes are transmitted by telmophagous blood-sucking tsetse flies (Lavoipierre, 1965) which are native in endemic areas in sub-Saharan Africa. Infection is characterized by a local swelling and migration of trypanosomes into the lymphatic fluid and blood. During this first hemo-lymphatic stage, common symptoms are a general malaise with a typical swelling of the lymph nodes (Winterbottom's sign), pain in head, joints and muscles and occasionally increased body temperature (Ross and Thomson, 1910). One of the early hallmarks during infection is transmigration of trypanosomes across the blood-cerebrospinal fluid barrier (BCB). Electron microscopy revealed that the parasite occurs in the stroma of the choroid plexus (Wolburg et al., 2012) before penetrating the plexus epithelial cell layer to enter the cerebrospinal fluid (CSF). This infiltration may repeat periodically following the oscillating blood parasitemia (Mogk et al., 2014b). However, the underlying mechanism remains to be investigated. The parasite spreads with the floating CSF within the ventricle system and settles inside the meninges, especially the *pia mater* (Mogk et al., 2014a; Wolburg et al., 2012). This stage has previously been referred to as ventricular meningeal stage (Mogk et al., 2016). It seems that the adjacent *glia limitans superficialis* stops the parasite's movement preventing an immediate infiltration of the neuropil, also called brain parenchyma. Instead, the parasite may follow the Virchow-Robin-space, a small cavity between the neuropil and the endothelium of near-surface blood vessels that reach into deeper brain areas. Either the parasite finally manages to cross the *glia limitans superficialis* (beneath the *pia mater* and surrounding the Virchow-Robin-space), or it invades the neuropil across the blood-brain barrier (BBB) which is formed by capillary endothelial cells interconnected by tight junctions. The barrier phenotype is maintained and modified by a basal lamina called *glia limitans perivascularis* and astrocyte endfeet. It was shown that transmigration across the BBB can occur very quickly in the case of extremely high parasitemia (Frevert et al., 2012), but it has also been described that the parasite will not survive nor develop inside the neuropil (Bafort et al., 1987; Mogk et al., 2014b; Schmidt and Bafort, 1985). This might be because of activated microglia that keep the illness in check (Figarella et al., 2018). Thus, it has been argued that infestation of the neuropil (the encephalitic stage) follows the meningeal stage with some delay, maybe after years (Mogk et al., 2016). In any case, during the encephalitic stage severe and life-threatening symptoms such as confusion, coordination difficulties, sensory impairment, epileptiform spasms, apathy and cachexia

[1]Interfaculty Institute of Biochemistry, University of Tübingen, Tübingen, Germany

[2]Department of Neurophysiology, University of Tübingen, Tübingen, Germany

[3]Laboratory of Clinical Regenerative Medicine, Department of Neurosurgery, Faculty of Medicine, University of Tsukuba, Tsukuba, Japan

[4]Pediatric Infectious Diseases, Department of Pediatrics, Medical Faculty Mannheim, Heidelberg University, Mannheim, Germany

[5]Lead contact

*Correspondence: stefan.mogk@uni-tuebingen.de

https://doi.org/10.1016/j.isci.2022.104014

occur (Brun et al., 2010). In addition, there is a dysregulation of the sleep-wake cycle leading to somnolence during daytime and insomnia at night. The progress of the disease usually extends over years (*T. brucei gambiense*) or months (*T. brucei rhodesiense*) and is thought to be lethal if untreated. However, rare cases of silent carriers have been described in literature, which had a chronic, but asymptomatic infection lasting for years or even decades (Alvar et al., 2020; Franco et al., 2014; Sudarshi et al., 2014; Welburn et al., 2016; Wurapa et al., 1984).

The parasite has a complex life cycle (Brun et al., 2010) with several morphologically and biochemically distinguishable stages in the tsetse fly as well as in mammals. With the insect taking a blood meal from an infected mammal it incorporates trypanosomes. Among them is a so-called "short stumpy" form, which is preadapted to the tsetse fly. Inside the midgut and proboscis of the fly, these stumpy trypanosomes develop to the procyclic (PC) stage (Brun et al., 2010). The cells enter the cell cycle and, after a few days, migrate through the peritrophic membrane and move headward within the ectoperitrophic space. From here, they re-enter the proventriculus and finally colonize the salivary glands (Aksoy, 2019). Although all other stages are trypomastigote, i.e., the flagellum originates at the end of the cell (behind the nucleus), an epimastigote form develops in the salivary gland characterized by the flagellum origin laying in the middle of the cell in front of the cell nucleus. Epimastigote parasites attach to the salivary glands' epithelium and develop into the metacyclic stage that is infectious to mammals. Being transmitted, metacyclic trypanosomes will spontaneously differentiate to so-called "long slender" form parasites, which are populating the host by proliferation in blood, lymph or tissue. To prevent the host's premature death from uncontrolled parasitic growth, the parasite secretes a stumpy induction factor (SIF) which induces differentiation of proliferating slender parasites into the cell cycle arrested "short stumpy" form (Hamm et al., 1990; Reuner et al., 1997; Rojas et al., 2019; Seed and Black, 1997). On the one hand, this can be interpreted as an altruistic cell density control, since stumpy trypanosomes secrete prostaglandin D2, an autocrine inductor of apoptosis in the stumpy parasite itself (Duszenko et al., 2006; Hamm et al., 1990). On the other hand, the stumpy form is preadapted to change hosts, as it will transform into procyclic trypanosomes as described above. During this process, variant surface glycoprotein (VSG) is shed with the help of major surface metalloprotease B and phospholipase C, and replaced by procyclin (de Sousa et al., 2010; Grandgenett et al., 2007; Gruszynski et al., 2006). As tissue invading cells are known to secrete metalloproteases to open tight junctions (Kleiner and Stetler-Stevenson, 1999), stumpy form trypanosomes had been proposed to be the "door-openers" who facilitate the transmigration across the BCB (Mogk et al., 2016). However, of course, many other proteases may be involved, among them prolyl oligopeptidase (TbPOP) and pyroglutamyl peptidase (TbPGP), which were recently identified to release SIF peptides (Rojas et al., 2019). Another candidate is the cysteine protease brucipain (cathepsin L), which seems to mediate transmigration across an *in vitro* model of the BBB (Grab et al., 2009; Nikolskaia et al., 2006).

Although the proteolytic opening of tight junctions is regarded important for transmigration, mechanical forces provoked by the flagellated parasite may also be involved. In this context, it is interesting to note that trypanosomes isolated from brain have been described as very long and slender (Schmidt and Bafort, 1987; Wolburg et al., 2012), and that the dominating population of trypanosomes inside the CSF was characterized by their fast and straight swimming behavior (Mogk et al., 2014a; Wolburg et al., 2012). As reported previously, trypanosomes cannot survive in human or rat CSF, even if potentially lacking nutrients are supplemented because of a thus far unknown trypanotoxic factor within CSF (e.g., neuropeptides) (Pentreath et al., 1992; Wolburg et al., 2012). Thus, highly motile trypanosomes may have a better chance to escape from this hostile environment to reach the *pia mater* (Wolburg et al., 2012), but cell geometry and motility may also affect transmigration efficiency. Slender and fast trypanosomes in blood would have better chances to invade the ventricle system. If so, being named after their appearance as drilling bodies (from the Greek words *trypanon* and *soma*) trypanosomes would make their name fully justified.

In vitro models of the BBB used human brain microvascular endothelial cells to analyze transmigration efficiency of *Trypanosoma brucei rhodesiense* and *T.b.brucei* (bloodstream and procyclic form) (Grab and Kennedy, 2008; Grab et al., 2004). In contrast, comparable studies are missing for the BCB, although an appropriate *in vitro* model is available and has been successfully applied to elucidate bacterial invasion (Dinner et al., 2016; Schwerk et al., 2012): Human epithelial choroid plexus papilloma cells (HIBCPP), which have originally been described by Ishiwata et al. (Ishiwata et al., 2005), are cultivated in a monolayer on permeable membranes (filter insert systems) to allow access to the apical and basolateral side of the cells. The filter membrane itself is available with different pore sizes (typically 0.4 μm or 3 μm) and mimics the
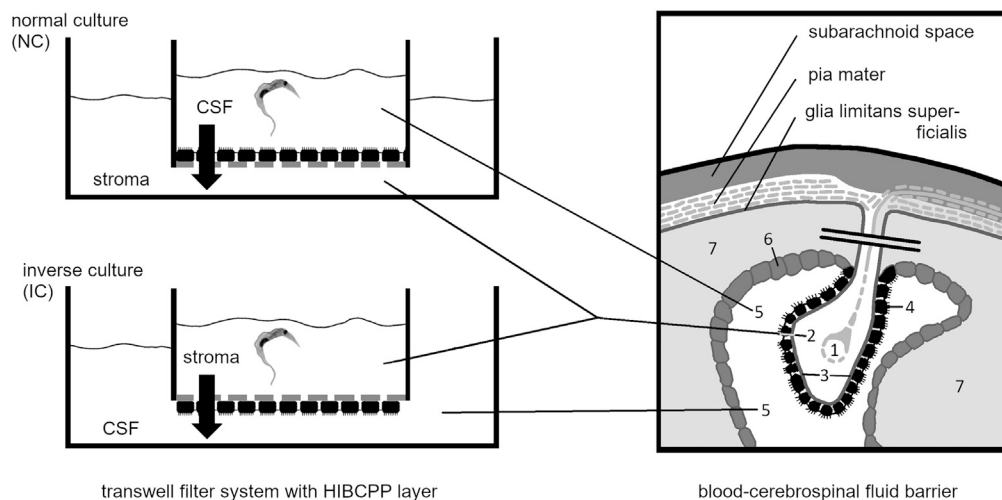
Figure 1. Anatomical structure of the choroid plexus and schematic representation of an *in vitro* BCB

The choroid plexuses are arteriovenous vascular convolutes in the ventricles of the brain. Its vessels (1) are built by a fenestrated capillary endothelium. Transmigrating cells (e.g., immune cells, bacteria or trypanosomes) penetrate into the surrounding connective tissue, the so-called plexus stroma (2). The stroma is demarcated from the ventricle lumen by a basal lamia (3) and a single layer of choroidal epithelium (4) whose apical surface faces the CSF (5). These plexus epithelial cells are interconnected by tight junctions, thus forming the BCB. The CSF-filled ventricles are lined out by an epithelium of ependyma cells (6), which separate CSF and brain parenchyma (also called neuropil, 7). To mimic the BCB *in vitro*, human choroid plexus papilloma cells are cultivated in a monolayer on a Transwell filter with 0.4, 3 or 8 μm pore size. The membrane mimics the basal lamina and allows the epithelial cells to polarize and interconnect by tight junction formation. Depending on whether the cells are sitting on top of the filter membrane (normal culture, NC) or hanging below the filter membrane (inverse culture, IC), the upper reservoir resembles the stroma of the choroid plexus (in case of IC) or the CSF-filled ventricle (in case of NC).

basal lamina allowing the choroid plexus epithelial cells to adhere. Under these conditions, HIBCPP cells express marker genes, polarize and interconnect by dense continuous tight junction strand formation, causing the development of a strong barrier function (Schwerk et al., 2012). Depending on whether the cells are sitting on top of the filter membrane (normal culture, NC) or hanging below the filter membrane (inverse culture, IC), the upper reservoir resembles the stroma of the choroid plexus (in case of IC) or the CSF-filled ventricle (in case of NC) (Figure 1). Integrity of the barrier function was monitored by measuring the flux of different tracer substances (radiolabeled sucrose, dye-labeled albumin, FITC-labeled inulin, or dye-labeled dextran) across the cell layer (Srinivasan et al., 2015). For a non-invasive monitoring of the barrier system the transepithelial electrical resistance (TEER) across the cell-layer was measured with commercially available (Schwerk et al., 2012) or self-made (Theile et al., 2019) voltammeters. We here describe how this *in vitro* model of the BCB can be used to compare transmigration efficiency of various trypanosome strains and defined differentiation stages. Applying fluorescent microscopy, the transmigration process was visualized.

RESULTS

Barrier function: correlation of electrical impedance and molecular flux

An *in vitro* BCB was set up as inverse culture. Therefore, cell culture PET filter inserts with a pore size of 3 μm and an area of 33 mm^2 were oriented upside down. HIBCPP cells were seeded to the bottom of the filter membrane. After 24h, cells had adhered, and the filters were turned into normal orientation. Thus, the upper compartment represented the stroma of the choroid plexus and the lower compartment the CSF (Figure 1). TEER was measured daily using a self-made voltammeter (Theile et al., 2019). Day 0 was defined when a filter reached 300 Ω (100 Ω·cm^2) and medium was changed to DMEM:F12 without serum. To assess barrier function, 22 mg/mL dextran blue (5 kDa molecular weight) was added to the upper reservoir. After 2 h, extinction of the medium in the lower wells was measured at 595 nm using a 96-well Dynex MRX plate reader. Dextran-free DMEM:F12 was used as reference. TEER and extinction values were correlated in Figure 2A. For each measurement, a new set of filters was used to prevent cell damage from repeated addition
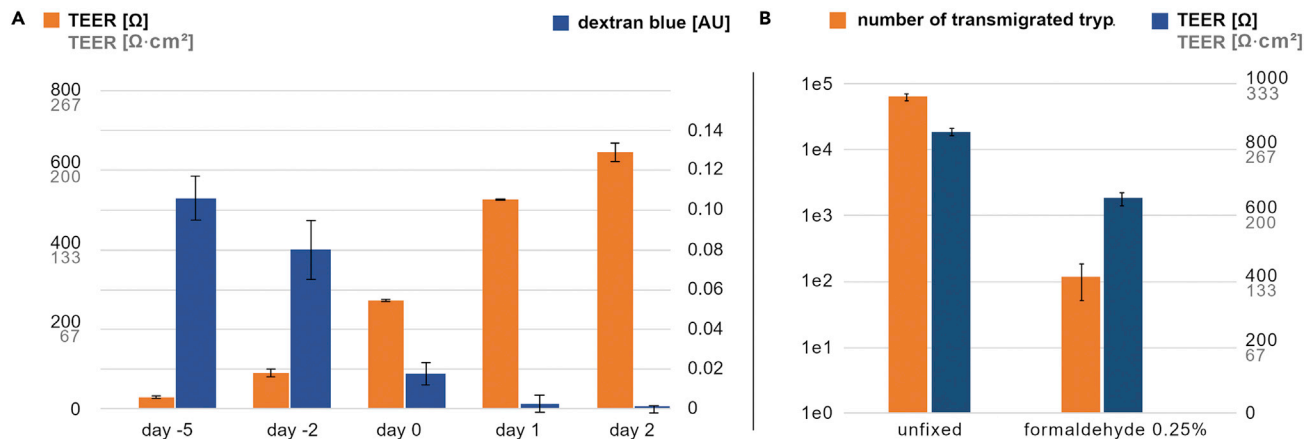
Figure 2. Barrier function of the *in vitro* BCB

(A) Molecular flux across the *in vitro* BCB. All filters were seeded as inverse culture. TEER was measured with a self-assembled voltammeter (orange, primary axis). At certain intervals, Dextran blue (5 kDa) in DMEM:F12 was added to the upper compartment to a final concentration of 22 mg/mL. After 2 h, extinction of lower compartment medium was measured at 595 nm against DMEM:F12 medium without dextran blue (blue, secondary axis). At each timepoint molecular flux was measured for two biological replicates (n = 2).

(B) Transmigration of live (positive control) or fixed (negative control) MiTat 1.2 VSG 221 trypanosomes. All filters were seeded as inverse culture. Filters for transmigration experiments were transferred to wells containing 1 mL HMI-9 medium and 5e6 MiTat 1.2 VSG 221 were added (in 500 μL HMI-9) to the upper compartment. For fixation, trypanosomes were incubated in 0.25% formaldehyde for 10 min and washed with TDB before applying to the respective filters. Transmigrated parasites were quantified after 2 h by qPCR with a primer set against alternative oxidase (TbAOX). Number of transmigrated cells is shown in orange (primary axis). TEER of HIBCPP filters before addition of trypanosomes is shown in blue (secondary axis). Data was measured for n = 2 biological replicates (each in 2 technical replicates). See also Figures S1C and S1D.

of dextran blue. If TEER reached 500 Ω (167 Ω·cm^2), extinction was only 2% of the value that was measured at day −5 (i.e., one day after the cells had been seeded). With higher TEER, dextran blue was not measurable, and filters were considered impermeable for high-molecular substances and cellular components. That should also be true for trypanosomes if there is no specific mechanism of penetration.

Quantification of transmigrated trypanosomes

T. brucei brucei were applied on the inverse filter insert in HMI-9 medium and moved (driven by gravity) to the lower well thus following the normal route of infection. Transmigrated parasites were quantified by qPCR. Attention was paid that detached and sedimented HIBCPP cells did not bias the results. Thus, a primer set against alternative oxidase (TbAOX) was chosen, a gene that is necessary for cellular respiration in *Trypanosoma brucei* and some other animal phyla (McDonald and Vanlerberghe, 2004) but absent in mammals. qPCR was tested with three different MiTat 1.2 VSG 221 trypanosome dilutions (1e6/mL, 1e5/mL, and 1e4/mL). The amplification plot showed that measurement was reproducible and melting curves suggested specific binding of the primer pair (Figures S1A and S1B). To check the reliability of this quantification method, we pipetted 5e6 MiTat 1.2 VSG 221 parasites (either alive or fixed with 0.25% formaldehyde) to the upper reservoir of the *in vitro* BCB and analyzed how much trypanosomal DNA could be found in the lower reservoirs after 2 h (Figure 2B). HIBCPP filters had a mean TEER of 853 ± 11 Ω (284 ± 4 Ω·cm^2, unfixed trypanosomes) or 650 ± 19 Ω (217 ± 6 Ω·cm^2, fixed trypanosomes). We measured a mean background of 117 ± 65 parasites in the negative (fixed) control, which represents approximately 2‰ of a typical transmigration result. This is most likely because of non-specific qPCR amplification (as indicated by the melting curves in Figures S1C and S1D). However, it is also possible that a small amount of medium from the upper chamber has passed along the outside of the filter into the lower chamber due to capillary action.

To verify that HMI-9 medium did not negatively impact barrier integrity, we moved a filter set with a mean TEER of 622 ± 41 Ω (207 ± 14 Ω·cm^2) into wells with 1 mL HMI-9 (lower reservoir). 500 μL HMI-9 were pipetted into the upper reservoir. TEER was measured after 1, 2, 4, 8 and 16h. As shown in Figure 3A, TEER remained constant and barrier function was considered to stay intact. In further experiments, we confirmed that the number of transmigrated parasites was dependent of the applied trypanosome concentration
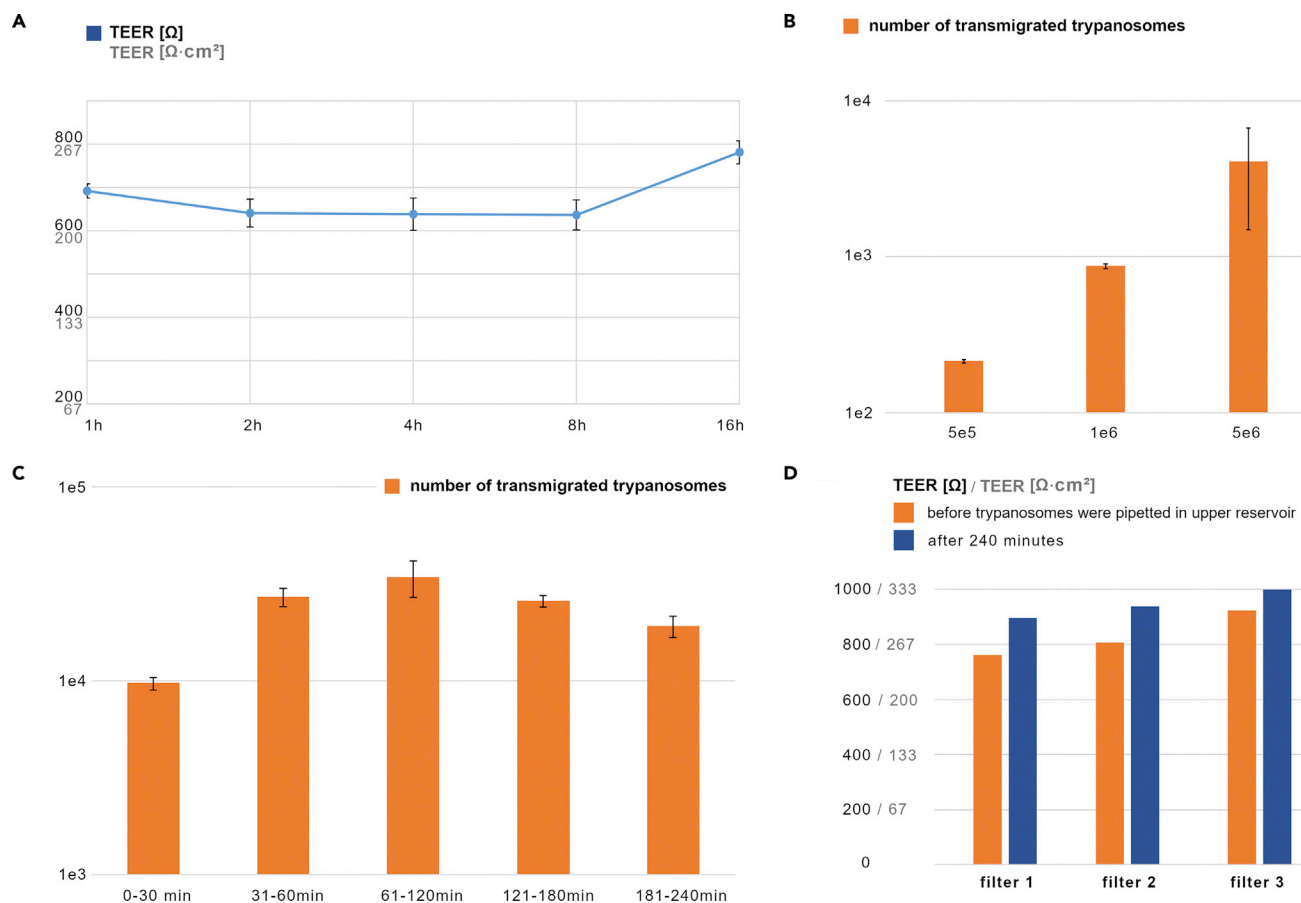
Figure 3. Stability of the *in vitro* BCB in HMI-9 medium and concentration/time dependency of the transmigration process

(A) Stability of the *in vitro* BCB in HMI-9 medium. All filters were seeded as inverse culture. When the filter set (n = 3 biological replicates) reached a mean TEER of 622 Ω (207 Ω·cm^2) (standard deviation 41 Ω), medium was changed to HMI-9. TEER was measured after 1, 2, 4, 8 and 16h. The start value (622 Ω at t = 0h) is not shown in the diagram because time is plotted logarithmically.
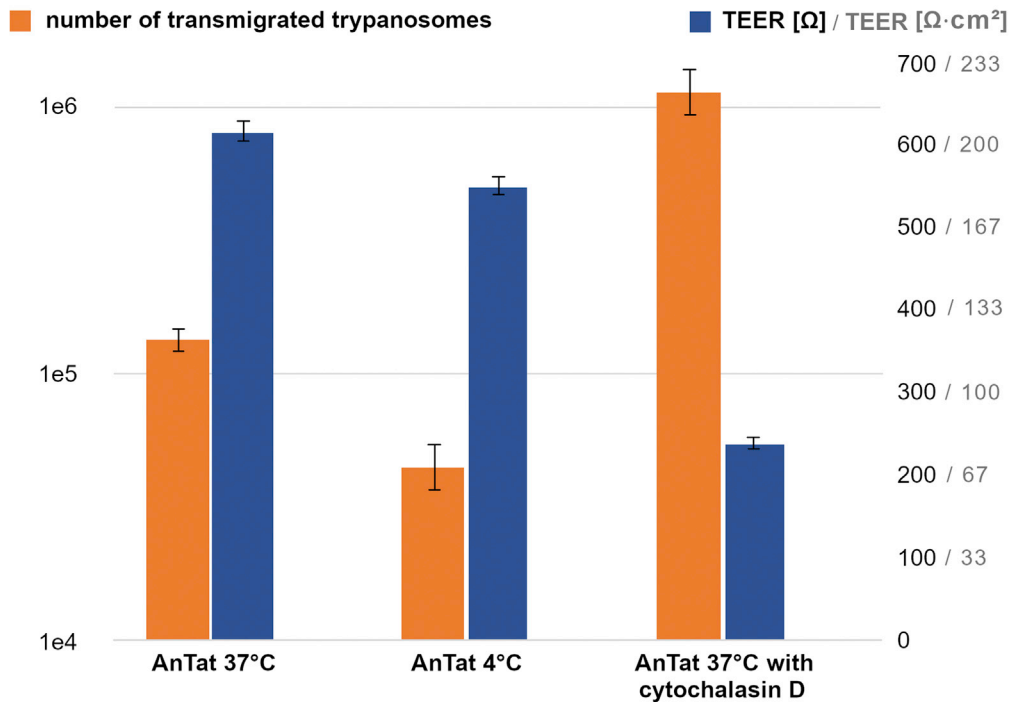
(B) Concentration dependency of transmigration across the *in vitro* BCB. All filters were seeded as inverse culture. For transmigration experiments the filters were transferred to wells containing 1 mL HMI-9 medium. 5e5, 1e6 and 5e6 MiTat 1.2 VSG 221 trypanosomes were added (in 500 μL HMI-9) to the upper compartment. After 30 min, the number of transmigrated parasites was quantified by qPCR with a primer set against alternative oxidase (TbAOX). Data was measured for n = 2 biological replicates per concentration (each in 2 technical replicates).

(C and D) Time dependent transmigration of MiTat 1.2 VSG 221. All filters were seeded as inverse culture. 5e6 trypanosomes were added (in 500 μL HMI-9) to the upper compartment. Data was measured for n = 3 biological replicates (each in 3 technical replicates). (C) Transmigrated parasites were quantified by qPCR with a primer set against alternative oxidase (TbAOX). (D) TEER was measured at the beginning (orange) and after (blue) the experiment.

(Figure 3B). 5e5, 1e6 and 5e6 MiTat 1.2 VSG 221 trypanosomes were added (in 500 μL HMI-9) to the upper compartment. After 30 min, the number of transmigrated cells was quantified by qPCR. We found a mean of 213 ± 5 parasites if 5e5 cells were applied, a mean of 867 ± 31 parasites for 1e6 applied cells and a mean of 4091 ± 2603 cells for 5e6 applied cells. Thus, no saturation effect could be observed for the parasite concentrations used in the manuscript. Analyzing transmigration kinetics, we added 5e6 trypanosomes (in 500 μL HMI-9) to the upper compartment. Transmigrated parasites were quantified by qPCR in several time intervals (0–30 min, 31–60 min, 61–120 min, 121–180 min and 181–240 min). After each time period, the filter inserts were moved to a new well containing 1 mL HMI-9 medium. The transmigration rate increased during the first 120 min, reaching a peak and then decreased again (Figure 3C). Measuring TEER before and after the experiment we found that the barrier function remained intact (Figure 3D).

Temperature-dependency of the transmigration process

For each transmigration experiment, filters with similar TEER were combined as biological replicates. Medium was changed to HMI-9, which supports survival of both trypanosomes and HIBCPP cells (Figure 3A).

Figure 4. Transmigration of pleomorphic trypanosomes (AnTat 1.1) at 37°C, 4 and 37°C with addition of cytochalasin D

All filters were seeded as inverse culture. Cytochalasin D was added to a final concentration of 1 µg/mL for 2 h before starting the transmigration experiment to disturb tight junction formation. Filters for transmigration experiments were transferred to wells containing 1 mL HMI-9 medium and 5e6 trypanosomes were added (in 500 µL HMI-9) to the upper compartment. Transmigrated parasites were quantified after 2 h by qPCR with a primer set against alternative oxidase (TbAOX). Number of transmigrated cells is shown in orange (primary axis). TEER of HIBCPP filters before addition of trypanosomes is shown in blue (secondary axis). Data is shown for n = 2 biological replicates (each in 2 technical replicates).p value was calculated with 1-way ANOVA as p = 3.8 e-6. See also Figure S2.

5e6 parasites were added to the ''stroma side'' (upper reservoir) of the *in vitro* BCB and incubated either at 37°C or 4°C. After 2 h, transmigrated trypanosomes were quantified by gDNA extraction and qPCR. As shown in Figures 4 and S2, transmigration was temperature-dependent suggesting an active process. We consider this plausible, as both motility (the drilling process when a trypanosome pushes itself through the HIBCPP cell layer) and enzyme activity (proteases that might be used to open tight junctions) decrease at low temperatures. As observed in light microscopy, flagellar movement slows down from some 18 Hz at 37°C (Heddergott et al., 2012) to approximately one beat per second at 4°C. Note that significantly ($p<0.001$) fewer trypanosomes transmigrated at 4°C ($4.5e4\pm9.9e3$) compared to 37°C ($1.3e5\pm1.2e4$), even though they had been pipetted on filters with lower TEER.
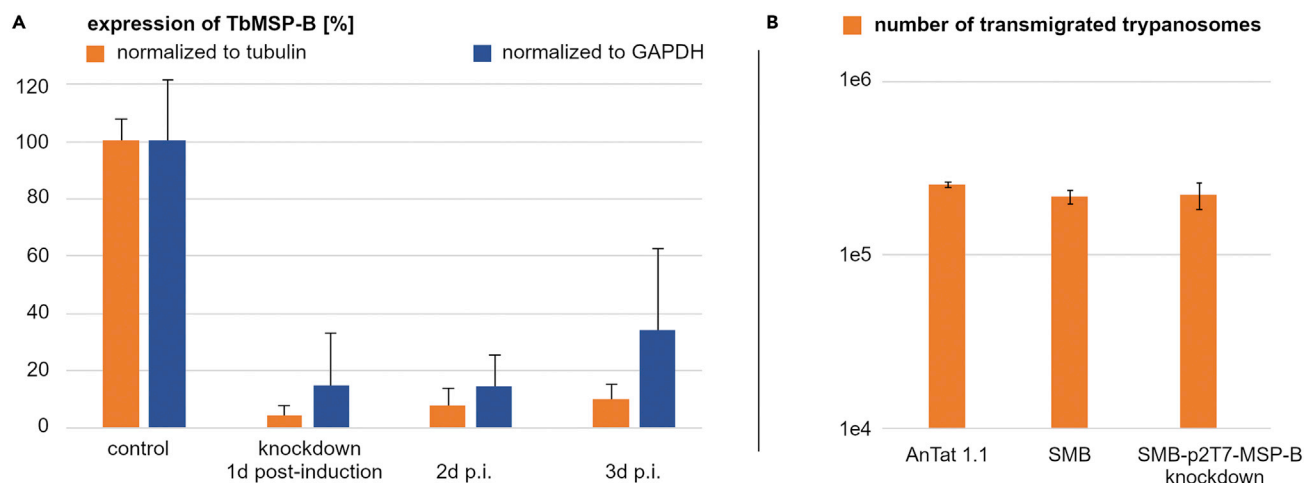
Opening of tight junctions allows transmigration

In general, the parasite can traverse the choroid plexus epithelium either para- or transcellularly. Regarding the size of trypanosomes and HIBCPP cells, a paracellular route seems more reasonable. That means an opening of tight junctions would be necessary to overcome the barrier. Actin polymerization (and thus tight junction formation) was inhibited by the addition of 1 µg/mL (final concentration) cytochalasin D (Stevenson and Begg, 1994; Vandenhaute et al., 2015) before loading the filters with trypanosomes. Within 2 h, TEER declined from approximately 600 (200 $\Omega\cdot cm^2$) to 250 Ω (83 $\Omega\cdot cm^2$) and transmigration efficiency increased nearly tenfold (i.e. from $1.3e5\pm1.2e4$ to $1.1e6\pm3.6e5$; Figures 4 and S2).

Transmigration of major surface metalloprotease B-deficient trypanosomes

An opening of tight junctions *in vivo* might be mediated by proteolytic digestion (as described for tissue invading cancer cells) or even by mechanical disruption, considering that tight junctions are dense, but not necessarily stable enough to withstand the leverage generated by the flagellar movement

A

expression of TbMSP-B [%]

■ normalized to tubulin ■ normalized to GAPDH

B

■ **number of transmigrated trypanosomes**

Figure 5. Transmigration efficiency of pleomorphic, monomorphic and TbMSP-B deficient trypanosomes

(A) Characterization of TbMSP-B knockdown cells (SMB-p2T7-MSP-B). Residual TbMSP-B mRNA was measured by quantitative reverse-transcriptase PCR. Expression level has been measured 1, 2 or 3 days after induction of RNA interference. Values have been normalized to different housekeeping genes, i.e. tubulin (orange) or GAPDH (blue). Data was measured for n = 3 technical replicates.

(B) Transmigration of culture-derived pleomorphic AnTat 1.1, monomorphic SMB and monomorphic TbMSP-B deficient (SMB-p2T7-MSP-B knockdown) trypanosomes. All filters were seeded as inverse culture. Filters for transmigration experiments were transferred to wells containing 1 mL HMI-9 medium and 5e6 trypanosomes were added (in 500 μL HMI-9) to the upper compartment. Transmigrated parasites were quantified after 2 h by qPCR with a primer set against alternative oxidase (TbAOX). Data was measured for n = 2 biological replicates (each in 2 technical replicates). There is no significant difference between the samples, p value was calculated with 1-way ANOVA as p = 0.191. See also Figure S3.

(Citi, 2019). It has been postulated that expression of major surface metalloprotease B (TbMSP-B) in stumpy trypanosomes facilitates BCB invasion. To check this assumption, a monomorphic TbMSP-B knockdown cell line was generated on basis of the SMB/p2T7 system (Alibu et al., 2005). SMB trypanosomes stably express T7 RNA polymerase and tetracycline repressor under neomycin resistance (T7RNAP TETR NEO). Part of TbMSP-B was cloned into p2T7 and is thus under control of two counter-oriented T7 promotors and tetracycline operators. The linearized vector was electroporated in SMB cells and integrated into the rDNA array via homologous recombination (RDNA::T7PRO^Ti MSP-B HYG). The resulting clonal TbMSP-B knockdown strain was characterized by qPCR (Figure 5A). Upon induction, dsRNA was transcribed, triggering RNA interference and degradation of TbMSP-B. After 1 day, 4% of residual mRNA was detected when normalized to tubulin mRNA, and 15% when normalized to GAPDH mRNA. Applying longer induction periods, mRNA level recovered to 8% (norm. to GAPDH: 15%) after 2 days and 10% (norm. to GAPDH: 34%) after 3 days. Growth curves revealed no difference between SMB control and TbMSP-B knockdown cells. However, no significant difference between both strains (SMB: 2.2e5±2.0e4, TbMSP-B kd: 2.3e5±4.9e4) was detected in the transmigration experiments (Figures 5B and S3). The result suggests that the role of MSP-B for tissue invasion has been overestimated, or that even a significantly reduced protease activity is sufficient to open tight junctions.

Comparison of bloodstream form and procyclic trypanosomes

It was reported that procyclic trypanosomes do not cross an *in vitro* model of the BBB (Grab and Kennedy, 2008). Interestingly, we found for the BCB that both procyclic and bloodstream form trypanosomes transmigrate (Figures 6 and S4). Transmigration occurred in two sets of experiments, one with a TEER of 700 Ω (233 Ω·cm^2) at the beginning of the experiment, and another where HIBCPP cells had formed multiple cell layers resulting in a higher TEER of 1700 Ω (566 Ω·cm^2). Although the latter does not represent the correct anatomical structure of the BCB (where the choroid plexus epithelium is single-layered), this result shows that the parasite is well adapted to the very compact tissue environment of the insect or vertebrate host (Doro et al., 2019). In each case, the transmigration rate was slightly higher for bloodstream form parasites than for fly-form parasites.

Importance of morphology for transmigration *in vitro*

Pleomorphic trypanosomes (AnTat 1.1) are fully capable to differentiate and naturally cause a long-term infection in mammals including a ventricular-meningeal stage. On the contrary, monomorphic parasites
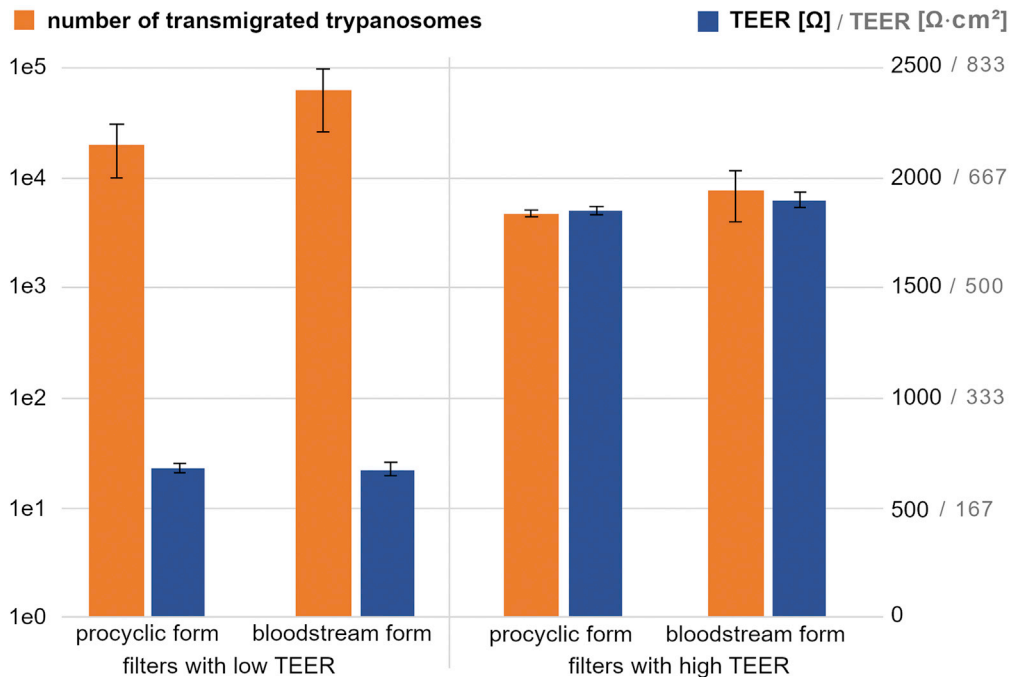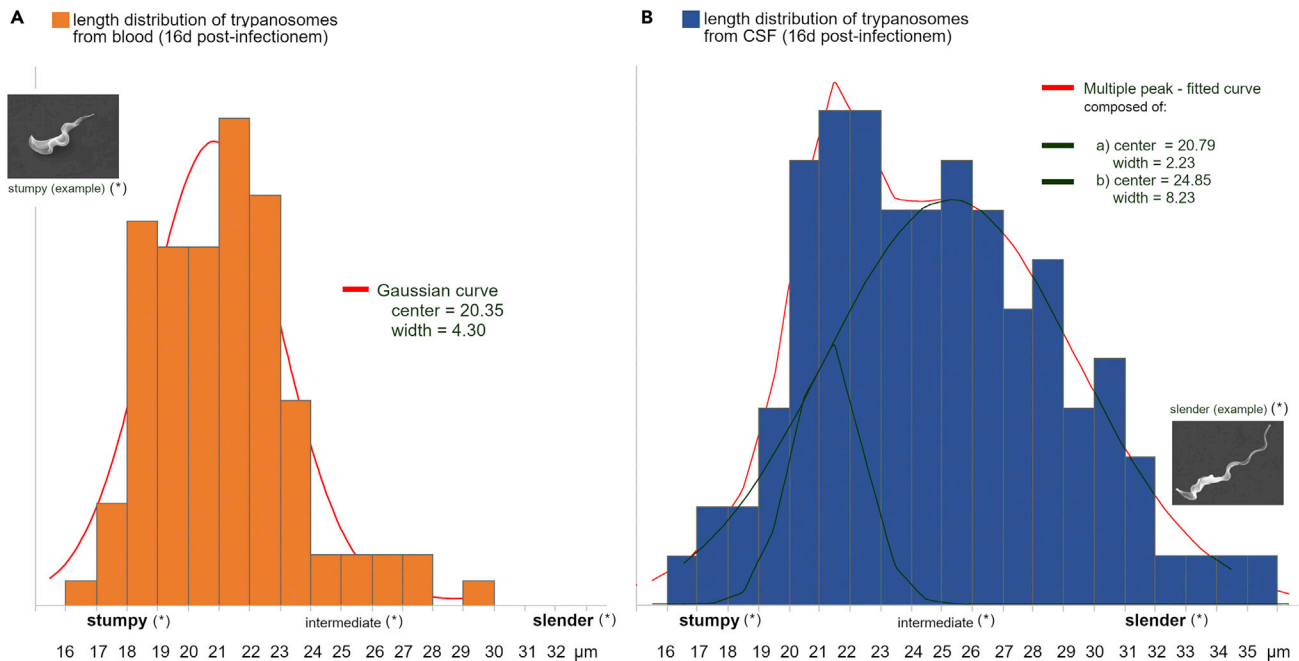
Figure 6. Transmigration of procyclic and bloodstream form trypanosomes

All filters were seeded as inverse culture. Filters for transmigration experiments were transferred to wells containing 1 mL HMI-9 medium and 5e6 trypanosomes were added (in 500 μL HMI-9) to the upper compartment. Transmigrated parasites were quantified after 2 h by qPCR with a primer set against alternative oxidase (TbAOX). Data was measured for n = 2 biological replicates. Left side: filter set with low TEER. Right side: filter set with high TEER (non-physiological model). Number of transmigrated cells is shown in orange (primary axis). TEER of HIBCPP filters before addition of trypanosomes is shown in blue (secondary axis). See also Figure S4.

(like MiTat 1.2 SMB) show unrestricted cell growth and kill the host within days before a brain infection becomes visible. However, if both strains are cultivated *in vitro* (in HMI-9 medium), their morphology appears to converge into what we describe as intermediate and stumpy cells, while there is no prominent long slender form visible. In case of *in vitro* cultivation, no significant difference in transmigration can be detected (Figures 5B and S3; AnTat: 2.7e5±8.9e3, SMB: 2.2e5±2.0e4). During an animal infection, however, AnTat 1.1 clearly shows all differentiation stages (stumpy, intermediate, and slender). In addition, a drift to longer parasites over time has been described (Mogk et al., 2012). Especially trypanosomes isolated from brain were reported as very long, slender, and highly motile (Mogk et al., 2014a; Wolburg et al., 2012). To draw conclusions on morphology-dependent transmigration efficiency, we have isolated parasites 16 days post-infection from rat blood and CSF by ventricle puncture (Mogk et al., 2014b). The flagellar length of hundred cells from each compartment has been measured as described elsewhere (Wolburg et al., 2012) (Figure 7). Although being derived from the same animal (at the same timepoint), trypanosomes that have entered CSF were on average significantly (p<0.001) longer than trypanosomes in blood. This is most probably because of the occurrence of two distinct populations (stumpy and slender morphology) in CSF (Figure 7B), whereas the blood sample at that timepoint contained only one (stumpy morphology) population (Figure 7A). We consider that long slender parasites cross the BCB more efficiently than stumpy cells, leading to an enrichment of cells which had not yet differentiated in CSF. As a result, there would be a delay of the differentiation process in CSF (compared to blood) with the occurrence of both slender and stumpy populations.

In preliminary experiments we compared the transmigration rate of monomorphic trypanosomes from cell culture and pleomorphic trypanosomes isolated from rat blood 23 days post-infection (Figure 8A). Trypanosome morphology was judged by microscopic observation: culture-derived cells contained no (or few) long slender trypanosomes. In contrast, blood-derived cells showed mostly a long slender morphology. Transmigration efficiency was significantly (p = 0.024) higher for blood-derived parasites

A length distribution of trypanosomes from blood (16d post-infectionem)

stumpy (example) (*)

Gaussian curve
center = 20.35
width = 4.30

stumpy (*)   intermediate (*)   **slender** (*)

16 17 18 19 20 21 22 23 24 25 26 27 28 29 30 31 32 μm

B length distribution of trypanosomes from CSF (16d post-infectionem)

Multiple peak - fitted curve
composed of:
a) center = 20.79
width = 2.23
b) center = 24.85
width = 8.23

slender (example) (*)

stumpy (*)   intermediate (*)   **slender** (*)

16 17 18 19 20 21 22 23 24 25 26 27 28 29 30 31 32 33 34 35 μm

Figure 7. Length distribution of different trypanosome populations (AnTat 1.1), which had been obtained from the same animal 16 days post-infection

Trypanosome length has been measured from anterior end to the flagellum tip

(A) Cells isolated from blood (n = 100) contained only one stumpy morphology population as shown in the histogram. A gaussian fit with a center of 20.35 and a width of 4.30 μm has been calculated with Origin.

(B) Cells isolated from CSF (n = 100) contained two distinct populations (stumpy and slender morphology). A multiple peak fitted curve (red) has been calculated with Origin, which is composed of two individual curves (green) with a center of 20.79 μm (width 2.23 μm) and 24.85 μm (width 8.23 μm), respectively. Representative surface electron microscopy images of a stumpy and a slender morphology parasite are given. Data published in (Mogk, 2014).

(*) Note that the terms "stumpy" and "slender" refer to the cell morphology and cells were not characterized by expression pattern analysis.

(MiTat/culture: 3.8e4 ± 1.4e4, AnTat/blood: 8.3e4 ± 2.4e4). As seen in other experiments (Figure 3D), TEER values have risen during the experiment, suggesting that the mechanism of transmigration does not induce a breakdown of barrier function (Figure 8B).

To demonstrate that transmigration becomes more difficult with increasing cell size, procyclic wildtype parasites were compared to a procyclic α-tubulin knockdown strain (parental strain MiTat 1.2 PC1313-514 (Alibu et al., 2005) electroporated with linearized p2T7-aTub; genotype TETR BLE T7RNAP NEO RDNA:: T7PRO^Ti ATUB HYG). This inducible knockdown leads to the inability to maintain the cellular structure and leads to the formation of balloon-shaped cells. As the knockdown efficiency was only about 50%, cells showing this so-called FAT phenotype were enriched on a cell culture filter insert with a pore size of 3 μm (without HIBCPP cells). *T.b.b.* cells without FAT phenotype passed the filter and were discarded (Figure 9A). For the *in vitro* BCB, we decided to use filter inserts with a pore size of 8 μm. The filter membrane itself did not sterically hinder trypanosomes from passing through (Figure 9B) (wildtype: 2.4e6 ± 2.1e5, alpha-tubulin kd: 3.5e6 ± 1.7e5). Thus, we conclude that the presorted cells with FAT phenotype had a diameter between 3 and 8 μm. If the barrier was formed by a HIBCPP layer, FAT phenotype cells had a much lower transmigration efficiency (p<0.001) than procyclic control cells (Figure 9B, 9C, and S5) (wildtype: 3.0e5 ± 1.5e4, alpha-tubulin kd: 1.5e4 ± 12.2e3).

The role of trypanosomal motility for CSF invasion

In trypanosomes, the flagellar beat leads to different ways of cellular movement. For example, movement can occur without net locomotion in so-called tumbling swimmers or with high locomotion in persistent (and directed) swimmers (Bargul et al., 2016). Trypanosomes isolated from CSF (or blood in late phase of infection) are highly motile, fast, and straight swimmers (Mogk et al., 2014a). Figure 10A and Video S1 give an impression of the swimming behavior of CSF-derived cells. It seems therefore possible that motility
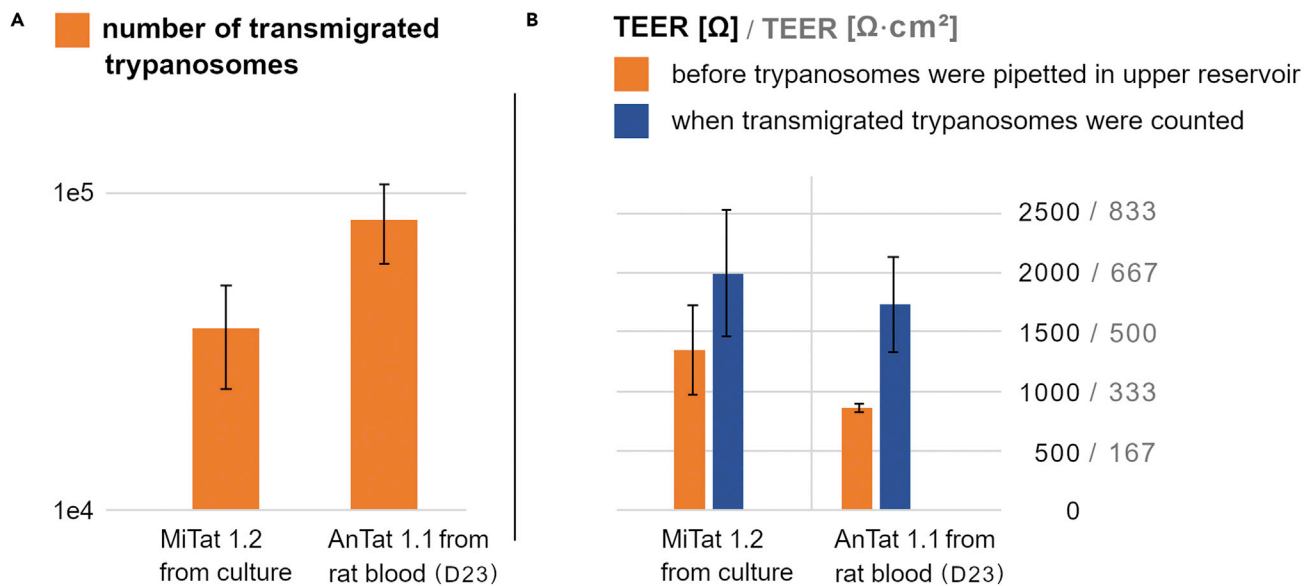
Figure 8. Transmigration of different trypanosome populations from culture or blood (preliminary data)

All filters were seeded as inverse culture. Filters for transmigration experiments were transferred to wells containing 1 mL HMI-9 medium and 1.5e5 trypanosomes were added (in 500 μL HMI-9) to the upper compartment. Transmigrated parasites were quantified after 16 h with a Neubauer improved counting chamber.

(A) Comparison of monomorphic trypanosomes from cell culture (MiTat 1.2, n = 5 biological replicates) and pleomorphic trypanosomes from rat blood 23 days post-infection (AnTat 1.1, n = 3 biological replicates). p value was calculated with 1-way ANOVA as 0.024.

(B) TEER of the *in vitro* BCB at the beginning of the experiment is shown in orange and after 16 h in blue. Data published in (Mogk, 2014).

might also influence transmigration efficiency. To test this hypothesis, we paralyzed procyclic trypanosomes with ciliobrevin A, a small molecule inhibitor of the AAA+ ATPase dynein. It must be noted that the motility-inhibiting effect of ciliobrevin A on bloodstream-form parasites is (possibly because of the VSG coat) much lower than on procyclic trypanosomes. However, as both bloodstream-form and procyclic trypanosomes cross the *in vitro* barrier, we assume that the results can be transferred to the bloodstream-form. As shown in Video S2, the inhibition of dynein-dependent microtubule gliding (and thus flagellar movement) is fully reversible when ciliobrevin is removed. Procyclic cells were pre-incubated in trypanosome dilution buffer (PBS with glucose) with or without ciliobrevin A before the suspension was pipetted to the upper reservoir of a Transwell filter insert without HIBCPP cells (which do not tolerate ciliobrevin). As in all transmigration experiments, the lower reservoir was filled with HMI-9 medium. After 15 or 40 min, respectively, transmigrated cells were quantified. As shown in Figures 10B and S6, a reduced motility significantly (15min: p = 0.017, 40min: p = 0.016) lowered transmigration efficiency across the filter membrane (15min control: 1.2e5±3.2e4, 15min ciliobrevin: 2.7e4±1.2e4, 40min control: 5.6e5±1.0e5, 40min ciliobrevin: 2.7e5±1.6e4)

Immunostaining/SEM of fixed filter membranes and live-cell imaging of the transmigration process

To visualize trypanosomes within the HIBCPP layer we incubated MiTat 1.2 VSG 221 on *in vitro* BCBs. For this monomorphic parasite, an anti-VSG antibody is available. Filter membranes have been fixed and immune-stained. Figure 11 shows a Z-Stack of a paracellular trypanosome in red, actin network of HIBCPP cells in green and nuclei in blue. As the staining procedure involves several washing steps, there were no sedimented trypanosomes on the filter membrane left, and only parasites, which were tightly dug within the epithelial cell layer remained in place. Additionally, we performed surface electron microscopy with view on the bottom side of the inverse culture. Figure 11 shows a trypanosome which just penetrated the barrier. In the background HIBCPP cells are clearly visible showing 9 + 0 cilia that are typically non-motile except for a perinatal period (Narita and Takeda, 2015).

To get a more dynamic view, we recorded the transmigration process in real-time. Thus, we performed live-cell imaging with the mCherry-expressing pleomorphic trypanosome strain GVR35 (MCHERRY PURO). To
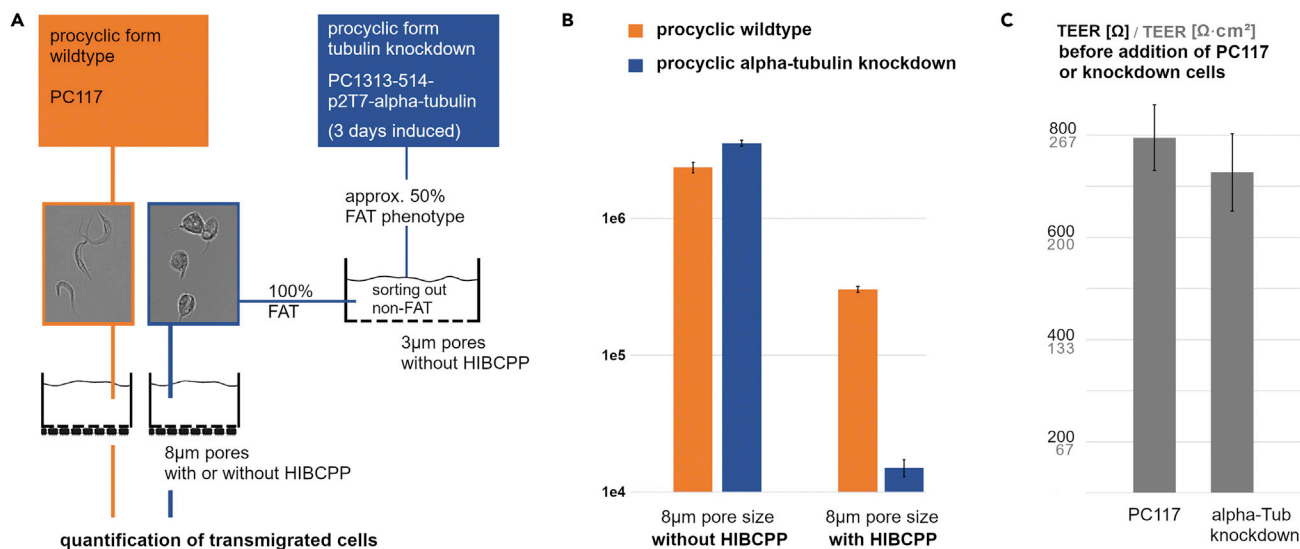
Figure 9. Transmigration of procyclic wildtype trypanosomes (PC117) and tubulin-deficient trypanosomes with FAT phenotype (PC1313-514-p2T7-alpha-tubulin)

(A) Schematic illustration of the experimental setup: PC117 control cells were directly applied to 8 μm pore size filters with HIBCPP cells (inverse culture) or without HIBCPP cells. Tubulin knockdown cells were induced for 3 days. FAT phenotype cells were then enriched on 3 μm pore size filters. The resulting population was applied to 8 μm pore size filters with HIBCPP cells (inverse culture) or without HIBCPP cells.

(B) All filters were seeded as inverse culture. Filters for transmigration experiments were transferred to wells containing 1 mL HMI-9 medium and 5e6 trypanosomes were added (in 500 μL HMI-9) to the upper compartment. Transmigrated parasites were quantified after 2 h by qPCR with a primer set against alternative oxidase (TbAOX). Transmigrated wildtype parasites are shown in orange; tubulin knockdown cells are shown in blue. Data was measured for n = 3 biological replicates. Between controls without HIBCPP cells there is no significant (p = 0.2452) difference in transmigration rate, between samples with HIBCPP cells there is a significant difference (p = 0.0004). See also Figure S5.

(C) TEER of HIBCPP filters before addition of trypanosomes (n = 3).

make HIBCPP cells visible, we used a commercially available live-cell plasma membrane stain. Videos S3 and S4 show parasites moving paracellularly between plexus epithelial cells. Several trypanosomes can be seen stuck between two cells. They seem to apply mechanical force before movement becomes suddenly possible again.

DISCUSSION

To form an *in vitro* BCB, choroid plexus epithelial cells are adhered to the bottom side of cell culture filter inserts. The filter membrane mimics a basal lamina and allows the HIBCPP cells to polarize. In inverted orientation, the upper reservoir resamples the stroma side of the choroid plexus and the lower reservoir the CSF side (Figure 1). TEER measurement (Theile et al., 2019) indicated when the cell layer was confluent and cells were interconnected by tight junctions. In addition, we measured the permeability to judge if the barrier function was intact. Therefore, we pipetted dextran blue to the upper reservoir and measured the extinction of the lower reservoir after 2 h against a dextran-free medium reference. The extinction one day after seeding the cells was defined as 100%. If TEER reached 500 Ω (166 Ω·cm²), the extinction decreased to 2%. For TEER values higher than 600 Ω (200 Ω·cm²), dextran blue was no longer detectable (Figure 2A). Because living (but not formaldehyde-fixed) *Trypanosoma brucei* could readily cross the barrier at a TEER higher than 600 Ω (200 Ω·cm²), this *in vitro* system is not limited to the elucidation of bacterial invasion (Schwerk et al., 2012) but can also be applied to analyze transmigration of eukaryotic cells (Figure 2B). After isolation of total DNA, the number of transmigrated cells was quantified by qPCR using a primer pair against trypanosomal alternative oxidase (TbAOX). This method gives high sensitivity and is specific for the parasite as AOX is absent in HIBCPP cells. Transmigration experiments with trypanosomes were performed in HMI-9 medium, which does not negatively impact barrier function (Figure 3A). The number of transmigrated parasites is dependent on the trypanosome concentration in the upper reservoir (Figure 3B). Thus, all Transwell filters within an experimental setup were loaded with an equal number of parasites. Transmigration rate was found to increase during the first 120 min, reaching a peak and then decreased again (Figure 3C). It must be noted that in the initial phase trypanosomes are in suspension and need
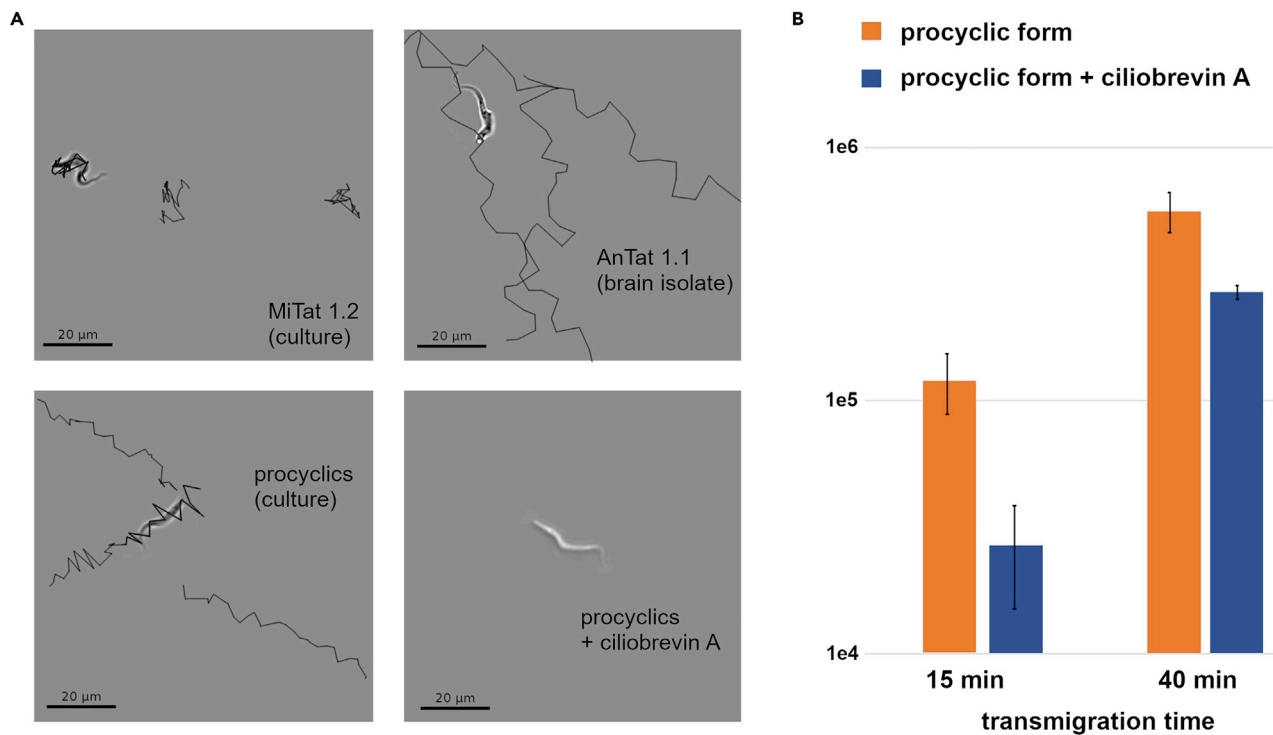
Figure 10. Relationship between motility and transmigration

(A) Trypanosomes were filmed with 10 frames/s, the position of the posterior end was marked in 30 frames and plotted to a path in one combined layer. Comparison of movement patterns of different trypanosome strains or stages (upper left: culture-derived MiTat 1.2, upper right: brain-isolated AnTat 1.1, lower left: culture-derived procyclics, lower right: ciliobrevin A-paralyzed procyclics). The path shows the distance travelled within 3s. Data partly published in (Mogk, 2014).

(B) Procyclic cells were preincubated for 15 min in PBS/20mM glucose with or without 500µM ciliobrevin A and transferred to the upper reservoir of a Transwell filter insert (3 µm pore size) without HIBCPP cells. The lower reservoir contained 1 mL HMI-9 medium. Transmigrated parasites were quantified after 15 min or 40 min by qPCR with a primer set against alternative oxidase (TbAOX). The number of transmigrated procyclic form trypanosomes without ciliobrevin A is shown in orange; with ciliobrevin A is shown in blue. Data was measured for n = 3 biological replicates. A reduced motility significantly (15min: $p = 0.017$, 40min: $p = 0.016$) lowered transmigration efficiency. See also Figure S6.

some time to sediment. As judged by TEER measurements, barrier function remained intact throughout a transmigration experiment (Figure 3D).

Transmigration is an active process, involving flagellar movement and/or proteolytic activity. We showed that low temperatures (4°C) prevent the parasite from crossing the HIBCPP cell layer (Figure 4). We consider a paracellular migration more likely than a transcellular migration, as 1) there is no intracellular stage described for *T.brucei* (in contrast to *T.cruzi* (de Souza et al., 2010)) and 2) trypanosomes (15– 35 µm in length, 1–5 µm in width) and plexus epithelial cells (10–15 µm in diameter (Liddelow et al., 2010)) are quite similar in size. Because some specialized cells, such as leukocytes, are able to migrate transcellularly despite their size (Steinmann et al., 2013), we cannot definitely exclude the transcellular route for trypanosomes, but found no hints to support it. Paracellular migration makes the tight junctions interconnecting the epithelial cells the main obstacle for invading trypanosomes. Destruction of tight junctions by cytochalasin D increased transmigration efficiency by factor 10 (which does not formally rule out that some parasites still cross transcellularly or take a combination of both routes) (Figure 4). Tissue-invading cells, e.g. metastatic cancer cells, use metalloproteases to overcome tight junctions (Kleiner and Stetler-Stevenson, 1999). Consequently, attention has been paid to whether trypanosomes also use proteases for tissue invasion: 1) the cysteine protease brucipain (cathepsin L, a lysosomal protein) has been associated with transmigration across the BBB (Grab et al., 2009); and 2) TbMSP-B, an enzyme used by stumpy form trypanosomes to release VSG was considered to be involved in digesting claudins (Mogk et al., 2016). Since coat-less trypanosomes were demonstrated within plexus stroma, the idea was that stumpy parasites die while exercising their function as "door-opener" for slender trypanosomes (Mogk et al., 2016). However,
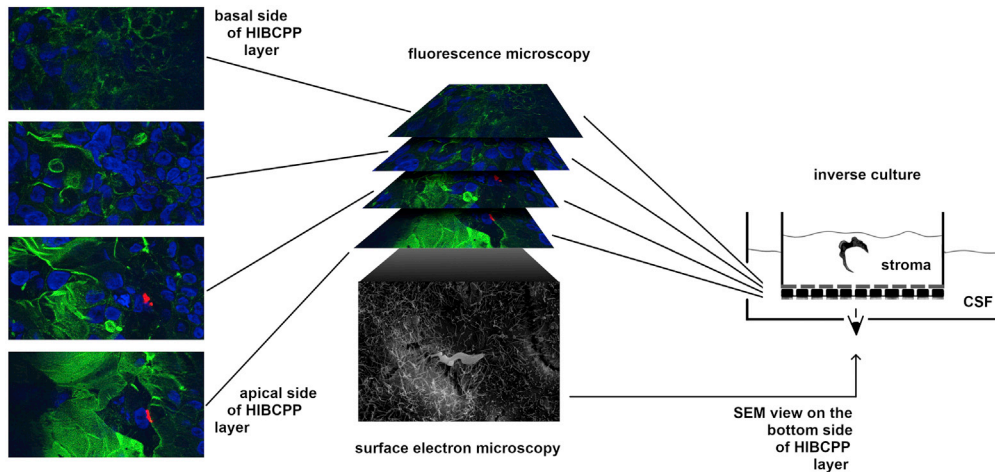
Figure 11. Imaging of monomorphic trypanosomes (MiTat 1.2) on an inverse culture BCB with 3 μm translucent filter inserts

Filters were fixed with paraformaldehyde and stained with rabbit anti-221/anti-rb-AF594, phalloidin-AF 488 and bisbenzimide or embedded for surface electron microscopy. Left: immune fluorescence microscopy (ApoTome Z-stack imaging) with trypanosomes in red, actin in green and nuclei in blue. Middle: surface electron microscopy of a transmigrated cell with view from bottom side of the HIBCPP layer.

using the *in vitro* BCB, we detected no difference in transmigration comparing wildtype and MSP-B-knock-down strains (Figure 5). In this context it needs to be reconsidered which kind of protease is eligible as a candidate for the opening of tight junctions. Contact time between integral membrane proteins (as MSP-B) and tight junction components can be expected to be very short as trypanosomes are fidgeting cells (unless they are trapped between plexus cells). Thus, it might be reasonable to extend the search to parasitic oligopeptidases, e.g., those known to generate the quorum sensing signal (Rojas et al., 2019). Notably, the effect of a transmigration-relevant protease seems to be paracrine only since TEER did not decrease during the experiments and the barrier function remained intact (Figure 3D).

In focusing on proteolytic activity, a mechanical disruption of the tight junctions was probably underestimated. It is textbook knowledge that tight junctions are extremely dense. Their function can be compared to a gate that limits the free movement of lipids, proteins and other solutes between the apical and the basolateral side (Narita and Takeda, 2015). Tight junctions are built by a network of non-covalently cross-linked transmembrane proteins of the claudin family (Fisher and Peppas, 2008). Specifically, in choroid plexus epithelial cells claudin-1/2/3/9/11/19/22 have been detected (Narita and Takeda, 2015). Although claudins maintain this dense barrier, they are much less involved in the mechanical stability (Fisher and Peppas, 2008). Instead, the strength of cell-cell adhesion is mediated by adherens junctions (Fisher and Peppas, 2008), which regulate tensile forces (Tietz and Engelhardt, 2015). Whereas the dense and narrow tight junction strands of the BCB run around the entire circumference of the choroid plexus cells (Tietz and Engelhardt, 2015), the strong (but not tightly closing) adherens junctions are not necessarily circulating, but often point-shaped (*punctum adhaerens*). Thus, tensile, compressive and shear forces between cells can affect the function of tight junctions (Citi, 2019). Considering the size and thus the leverage that a trypanosome can apply, we guess it is possible that a parasite can bring the tip of the pulling flagellum between the HIBCPP cells and mechanically disrupt tight junctions, thus pushing the cells apart. Of course, a combination of proteolysis and mechanics is just as conceivable. As observed by live-cell imaging, paracellular parasites seemed temporarily stuck, applying mechanical force. Suddenly, they struggled themselves free to move back and forth between HIBCPP cells (Videos S3 and S4).

Contrary to previous observations made in an *in vitro* BBB (Grab and Kennedy, 2008; Grab et al., 2004), we found that both bloodstream form and procyclic trypanosomes were able to cross the HIBCPP layer of the BCB (Figure 6). The observed difference in transmigration efficiency might be because of a different expression pattern of relevant proteins (e.g., proteases) and/or because of differences in shape and swimming behavior. We hypothesize that the ability to migrate into tissues was an evolutionary invention, probably to hide out in immune-privileged habitats or to benefit from sleep induction in mammals, which allows
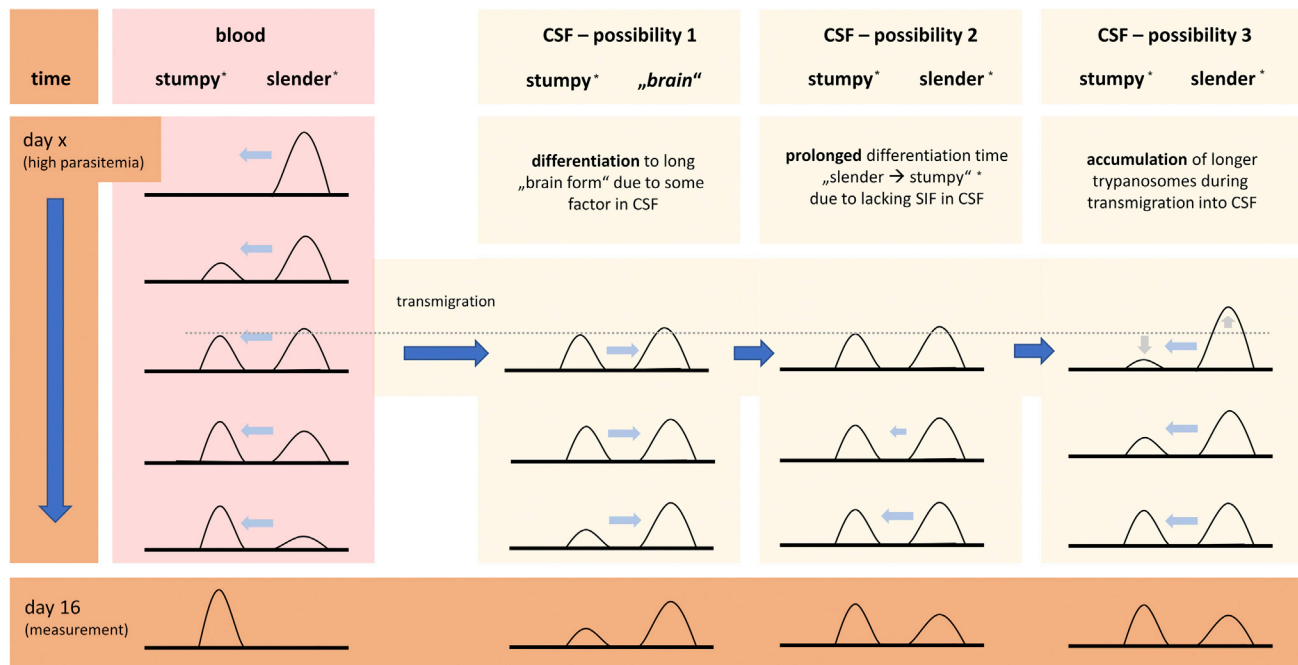
Figure 12. Presentation of different hypothesis to explain the occurrence of a single stumpy population in rat blood and two distinct (stumpy and slender) populations in rat CSF, as found in the same animal at the same timepoint (see Figure 7)

Possibility 1: An unknown factor in CSF could induce differentiation of invading stumpy cells into a long 'brain stage'. Possibility 2: As parasite density in CSF follows the blood parasitemia with some delay, invading cells could face an environment with a reduced SIF concentration. As a result, cell-density mediated differentiation from slender to stumpy could be already completed in blood but delayed in CSF. Possibility 3: Transmigration efficiency could be higher for slender cells than for stumpy cells. This would lead to an accumulation of slender cells in CSF. (*) Note that conclusions on "stumpy" and "slender" cells have been drawn by observation of the cell morphology, not by expression pattern analysis.

undisturbed biting of tsetse flies and transmission of trypanosomes. The parasite broadly uses this capability to extravasate, and invades a variety of organs (Mogk et al., 2014b) and tissues, e.g. skin and fat tissue (Capewell et al., 2016; Trindade et al., 2016), choroid plexus and meninges (Wolburg et al., 2012), circumventricular organs (Mogk et al., 2016; Schultzberg et al., 1988) and brain parenchyma (Frevert et al., 2012). Probably, there is no need for procyclic trypanosomes to cross epithelial barriers within the tsetse fly. Travelling from the tsetse midgut, trypanosomes seem to penetrate the soft part of the peritrophic membrane and move headward within the ectoperitrophic space. From here, they re-enter the proventriculus and finally colonize the salivary glands (Aksoy, 2019). However, some publications reported that trypanosomes do cross the midgut epithelium *in vivo* and occur within the hemolymph (Mshelbwala, 1972; Otieno et al., 1976). This might be of no physiological relevance as hemolymph contains trypanolytic substances (Croft et al., 1982), but it indicates that the ability to transmigrate is not exclusively limited to a single stage during the parasite's life cycle and would be consistent with our finding that procyclics cross the HIBCPP layer.

Surprisingly, monomorphic MiTat 1.2 and pleomorphic AnTat 1.1 did not differ in the transmigration rate if they were grown in culture, as the strains resemble each other in size and morphology during cultivation (Figure 5B). However, we noticed that when pleomorphic trypanosomes were propagated in the animal, the cells became longer and thinner with increasing infection duration (Mogk et al., 2012). In particular, many parasites present in the brain were reported to have a remarkably long slender morphology (Wolburg et al., 2012). Thus, we compared the length distribution of trypanosomes taken from different compartments (rat CSF and blood) at the same time (16 days post-infection) of the same animal. We observed a single stumpy morphology population with a mean cell length of 20.4 µm within blood, suggesting that all blood parasites had recently differentiated in response to a high parasitemia (Figure 7A). In CSF however, two distinct populations (stumpy and slender morphology, with a mean cell length of 20.8 and 24.9, respectively) occurred (Figure 7B). In general, this could be because of the CSF-mediated differentiation into a long 'brain stage' (Figure 12, possibility 1), which had been proposed in literature (Wolburg et al., 2012), but never characterized. Regarding that the increasing occurrence of longer forms during the course

Table 1. Overview of the trypanosome strains used, their properties, genotypes and antibiotic resistances

T.b.b strain	Characteristics	Genotype	Selective antibiotic
MiTat 1.2 VSG 221	monomorphic BSF	Wildtype	none
MiTat 1.2 SMB-p2T7-MSP-B	monomorphic BSF ("SMB")	T7RNAP TETR NEO RDNA::T7PRO^Ti MSP-B HYG	G418, hygromycin
AnTat 1.1E	pleomorphic BSF	Wildtype	none
GVR35-mCherry	pleomorphic BSF	MCHERRY PURO	puromycin
MiTat 1.2 PC117	PC	Wildtype	none
MiTat 1.2 PC1313-514-α-Tub	PC ("FAT phenotype")	TETR BLE T7RNAP NEO RDNA::T7PRO^Ti ATUB HYG	phleomycin, G418,hygromycin

BSF, bloodstream form; PC, procyclic form

of infection has been reported even in blood (Mogk et al., 2012), it is questionable if these cells originate from CSF. As parasite density in CSF is known to follow the blood parasitemia with some delay (Mogk et al., 2014b), transmigrated cells could face an environment with a reduced SIF concentration. This would lead to a prolonged differentiation time and could explain why we found a remaining slender morphology population in CSF (Figure 12, possibility 2). Finally, the occurrence of slender parasites in CSF could also be attributed to the transmigration efficiency being higher for long (and therefore thin) cells than for stumpy morphology cells. This would lead to an accumulation of slender cells and to a delay of the differentiation process in CSF (Figure 12, possibility 3). In the latter case, geometry would play an important role in penetrating cellular barriers.

In preliminary experiments we compared transmigration efficiency of cell culture-derived MiTat 1.2 with stumpy/intermediate morphology and blood-derived AnTat 1.1 (23 days after infection) with slender morphology (as judged by microscopic observation). We found that blood-derived parasites had a significantly higher transmigration efficiency (Figure 8A). This indicates that morphology is an important property for trypanosome invasion into CSF. This could also be confirmed when we tested alpha-tubulin deficient trypanosomes (FAT phenotype), which could hardly cross the *in vitro* barrier (Figure 9B).

Additionally, it has been reported that CSF-derived long slender trypanosomes are fast and persistent swimmers (Wolburg et al., 2012). This fits with the fact that a higher cell length allows faster locomotion due to a different flow resistance (Uppaluri et al., 2011). So, motility might be another important feature for CSF invasion. To test this hypothesis, we paralyzed trypanosomes with ciliobrevin A. This small molecule inhibits the AAA+ ATPase dynein which is responsible for microtubule gliding and flagellar movement. Ciliobrevin A reversibly slows down movement of leishmania (Reddy et al., 2017) and procyclic trypanosomes (Sun et al., 2018). Sun et al. state that coordinated flagellum-cell body movement is necessary to overcome synthetic obstacles (Sun et al., 2018). Consistently, we found that immobilized parasites are largely retained at the Transwell filter membrane itself (Figure 10). In summary, our results hint that shape and motility of the parasite are closely linked to its ability to invade tissues. More than that, even infectivity itself has been reported to be dependent on flagellar movement (Shimogawa et al., 2018).

The *in vitro* BCB presented here provides a simple tool to compare trypanosome strains for their ability to infect CSF, or to test the impact of chemical substances on transmigration. We consider it likely that this method will in future be suitable to efficiently screen CRISPR/cas9 or RNAi modified cell libraries and gain new insights into the genetic background that makes trypanosomal transmigration across the BCB possible.

Limitations of the study

This study has limitations. As in all *in vitro* models, the complex processes within a living system cannot be completely simulated. The tight junctions between HIBCPP cells were described to consist of meshed strands, whereas tight junctions in primary choroid plexus epithelial cells run in a parallel array (Schwerk et al., 2012). This could be because of a reduced expression of claudin 11 in HIBCPP cells. Contrary to primary choroid plexus epithelial cells, HIBCPP tend to form multilayers because of lost contact inhibition.

STAR★METHODS

Detailed methods are provided in the online version of this paper and include the following:

- KEY RESOURCES TABLE
- RESOURCE AVAILABILITY
  - Lead contact
  - Materials availability
  - Data and code availability
- EXPERIMENTAL MODEL AND SUBJECT DETAILS
  - *Trypanosoma brucei brucei* strains
- METHOD DETAILS
  - *In vitro* BCB
  - DNA/RNA purification
  - Quantitative PCR
  - Measurement of trypanosome motility
  - Imaging of HIBCPP filter membranes
  - Abbreviations
  - Ethics statement
- QUANTIFICATION AND STATISTICAL ANALYSIS
  - Statistical analysis

SUPPLEMENTAL INFORMATION

Supplemental information can be found online at https://doi.org/10.1016/j.isci.2022.104014.

AUTHOR CONTRIBUTIONS

S.M. designed, A.S., M.T., L.P., A.H. and S.M. performed the experiments. K.F., H.I., C.S. and H.S. contributed to materials and methodology. K.F., C.S., H.S. and M.D. provided intellectual input and critical feedback and commented on the manuscript. S.M. wrote and M.D. revised the manuscript.

DECLARATION OF INTERESTS

There are no conflicts to declare.

REFERENCES

Aksoy, S. (2019). Tsetse peritrophic matrix influences for trypanosome transmission. J. Insect Physiol. *118*, 103919. https://doi.org/10.1016/j.jinsphys.2019.103919.

Alibu, V.P., Storm, L., Haile, S., Clayton, C., and Horn, D. (2005). A doubly inducible system for RNA interference and rapid RNAi plasmid construction in *Trypanosoma brucei*. Mol. Biochem. Parasitol. *139*, 75–82. https://doi.org/10.1016/j.molbiopara.2004.10.002.

Alvar, J., Alves, F., Bucheton, B., Burrows, L., Buscher, P., Carrillo, E., Felger, I., Hubner, M.P., Moreno, J., Pinazo, M.J., et al. (2020). Implications of asymptomatic infection for the natural history

of selected parasitic tropical diseases. Semin. Immunopathol. *42*, 231–246. https://doi.org/10.1007/s00281-020-00796-y.

Bafort, J.M., Schmidt, H., and Molyneux, D.H. (1987). Development of *Trypanosoma brucei* in suckling mouse brain following intracerebral injection. Trans. R. Soc. Trop. Med. Hyg. *81*, 487–490.

Bargul, J.L., Jung, J., McOdimba, F.A., Omogo, C.O., Adung'a, V.O., Kruger, T., Masiga, D.K., and Engstler, M. (2016). Species-specific adaptations of trypanosome morphology and motility to the mammalian host. PLoS Pathog. *12*, e1005448. https://doi.org/10.1371/journal.ppat.1005448.

Brun, R., Blum, J., Chappuis, F., and Burri, C. (2010). Human African trypanosomiasis. Lancet *375*, 148–159.

Capewell, P., Cren-Travaille, C., Marchesi, F., Johnston, P., Clucas, C., Benson, R.A., Gorman, T.A., Calvo-Alvarez, E., Crouzols, A., Jouvion, G., et al. (2016). The skin is a significant but overlooked anatomical reservoir for vector-borne African trypanosomes. Elife *5*, e17716. https://doi.org/10.7554/eLife.17716.

Citi, S. (2019). The mechanobiology of tight junctions. Biophys. Rev. *11*, 783–793. https://doi.org/10.1007/s12551-019-00582-7.

Croft, S.L., East, J.S., and Molyneux, D.H. (1982). Anti-trypanosomal factor in the haemolymph of Glossina. Acta Trop. *39*, 293–302.

de Sousa, K.P., Atouguia, J., and Silva, M.S. (2010). Partial biochemical characterization of a metalloproteinase from the bloodstream forms of Trypanosoma brucei brucei parasites. Protein J. *29*, 283–289. https://doi.org/10.1007/s10930-010-9250-8.

de Souza, W., de Carvalho, T.M., and Barrias, E.S. (2010). Review on trypanosoma cruzi: host cell interaction. Int. J. Cell Biol. *2010*, 295394. https://doi.org/10.1155/2010/295394.

Dinner, S., Borkowski, J., Stump-Guthier, C., Ishikawa, H., Tenenbaum, T., Schroten, H., and Schwerk, C. (2016). A choroid plexus epithelial cell-based model of the human blood-cerebrospinal fluid barrier to study bacterial infection from the basolateral side. J. Vis. Exp. *6*, 54061. https://doi.org/10.3791/54061.

Doro, E., Jacobs, S.H., Hammond, F.R., Schipper, H., Pieters, R.P., Carrington, M., Wiegertjes, G.F., and Forlenza, M. (2019). Visualizing trypanosomes in a vertebrate host reveals novel swimming behaviours, adaptations and attachment mechanisms. Elife *8*, e48388. https://doi.org/10.7554/eLife.48388.

Duszenko, M., Figarella, K., Macleod, E.T., and Welburn, S.C. (2006). Death of a trypanosome: a selfish altruism. Trends Parasitol. *22*, 536–542. https://doi.org/10.1016/j.pt.2006.08.010.

Figarella, K., Uzcategui, N.L., Mogk, S., Wild, K., Fallier-Becker, P., Neher, J.J., and Duszenko, M. (2018). Morphological changes, nitric oxide production, and phagocytosis are triggered *in vitro* in microglia by bloodstream forms of *Trypanosoma brucei*. Sci. Rep. *8*, 15002. https://doi.org/10.1038/s41598-018-33395-x.

Fisher, O.Z., and Peppas, N.A. (2008). Quantifying tight junction disruption caused by biomimetic pH-sensitive hydrogel drug carriers. J. Drug Deliv. Sci. Technol. *18*, 47–50. https://doi.org/10.1016/s1773-2247(08)50006-2.

Franco, J.R., Simarro, P.P., Diarra, A., and Jannin, J.G. (2014). Epidemiology of human African trypanosomiasis. Clin. Epidemiol. *6*, 257–275. https://doi.org/10.2147/CLEP.S39728.

Frevert, U., Movila, A., Nikolskaia, O.V., Raper, J., Mackey, Z.B., Abdulla, M., McKerrow, J., and Grab, D.J. (2012). Early invasion of brain parenchyma by African trypanosomes. PLoS One *7*, e43913. https://doi.org/10.1371/journal.pone.0043913.

Grab, D.J., Garcia-Garcia, J.C., Nikolskaia, O.V., Kim, Y.V., Brown, A., Pardo, C.A., Zhang, Y., Becker, K.G., Wilson, B.A., de, A.L.A.P., et al. (2009). Protease activated receptor signaling is required for African trypanosome traversal of human brain microvascular endothelial cells. PLoS Negl. Trop. Dis. *3*, e479. https://doi.org/10.1371/journal.pntd.0000479.

Grab, D.J., and Kennedy, P.G.E. (2008). Traversal of human and animal trypanosomes across the blood-brain barrier. J. Neurovirol. *14*, 344–351.

Grab, D.J., Nikolskaia, O., Kim, Y.V., Lonsdale-Eccles, J.D., Ito, S., Hara, T., Fukuma, T., Nyarko, E., Kim, K.J., Stins, M.F., et al. (2004). African trypanosome interactions with an *in vitro* model of the human blood-brain barrier. J. Parasitol. *90*, 970–979.

Grandgenett, P.M., Otsu, K., Wilson, H.R., Wilson, M.E., and Donelson, J.E. (2007). A function for a specific zinc metalloprotease of African trypanosomes. PLoS Pathog. *3*, 1432–1445. https://doi.org/10.1371/journal.ppat.0030150.

Gruszynski, A.E., van Deursen, F.J., Albareda, M.C., Best, A., Chaudhary, K., Cliffe, L.J., del Rio, L., Dunn, J.D., Ellis, L., Evans, K.J., et al. (2006). Regulation of surface coat exchange by differentiating African trypanosomes. Mol. Biochem. Parasitol. *147*, 211–223. https://doi.org/10.1016/j.molbiopara.2006.02.013.

Hamm, B., Schindler, A., Mecke, D., and Duszenko, M. (1990). Differentiation of *Trypanosoma brucei* bloodstream trypomastigotes from long slender to short stumpy-like forms in axenic culture. Mol. Biochem. Parasitol. *40*, 13–22.

Haselbach, M., Wegener, J., Decker, S., Engelbertz, C., and Galla, H.J. (2001). Porcine choroid plexus epithelial cells in culture: regulation of barrier properties and transport processes. Microsc. Res. Tech. *52*, 137–152. https://doi.org/10.1002/1097-0029(20010101)52:1<137::AID-JEMT15>3.0.CO;2-J.

Heddergott, N., Kruger, T., Babu, S.B., Wei, A., Stellamanns, E., Uppaluri, S., Pfohl, T., Stark, H., and Engstler, M. (2012). Trypanosome motion represents an adaptation to the crowded environment of the vertebrate bloodstream. PLoS Pathog. *8*, e1003023. https://doi.org/10.1371/journal.ppat.1003023.

Ishiwata, I., Ishiwata, C., Ishiwata, E., Sato, Y., Kiguchi, K., Tachibana, T., Hashimoto, H., and Ishikawa, H. (2005). Establishment and characterization of a human malignant choroids plexus papilloma cell line (HIBCPP). Hum.Cell *18*, 67–72. https://doi.org/10.1111/j.1749-0774.2005.tb00059.x.

Kennedy, P.G.E. (2013). Clinical features, diagnosis, and treatment of human African trypanosomiasis (sleeping sickness). Lancet Neurol. *12*, 186–194.

Kleiner, D.E., and Stetler-Stevenson, W.G. (1999). Matrix metalloproteinases and metastasis. Cancer Chemother. Pharmacol. *43*, S42–S51.

Lavoipierre, M.M. (1965). Feeding mechanism of blood-sucking arthropods. Nature *208*, 302–303. https://doi.org/10.1038/208302a0.

Liddelow, S.A., Dziegielewska, K.M., Vandeberg, J.L., and Saunders, N.R. (2010). Development of the lateral ventricular choroid plexus in a marsupial, Monodelphis domestica. Cerebrospinal Fluid Res. *7*, 16. https://doi.org/10.1186/1743-8454-7-16.

McDonald, A., and Vanlerberghe, G. (2004). Branched mitochondrial electron transport in the Animalia: presence of alternative oxidase in several animal phyla. IUBMB Life *56*, 333–341. https://doi.org/10.1080/1521-6540400000876.

Mogk, S. (2014). Dissertation: Aufklärung des Infektionsweges der Gehirninfektion von Trypanosoma brucei und Charakterisierung der Parasiten im zentralen Nervensystem. University of Tuebingen, ISBN 978-3-7375-2828-3.

Mogk, S., Bosselmann, C.M., Mudogo, C.N., Stein, J., Wolburg, H., and Duszenko, M. (2016). African trypanosomes and brain infection - the unsolved question. Biol. Rev. Camb. Philos. Soc. *92*, 1675–1687. https://doi.org/10.1111/brv.12301.

Mogk, S., Meiwes, A., Bosselmann, C.M., Wolburg, H., and Duszenko, M. (2014a). The lane to the brain: how African trypanosomes invade the CNS. Trends Parasitol. *30*, 470–477. https://doi.org/10.1016/j.pt.2014.08.002.

Mogk, S., Meiwes, A., Shtopel, S., Schraermeyer, U., Lazarus, M., Kubata, B., Wolburg, H., and Duszenko, M. (2014b). Cyclical appearance of african trypanosomes in the cerebrospinal fluid: new insights in how trypanosomes enter the CNS. PLoS One *9*, e91372. https://doi.org/10.1371/journal.pone.0091372.

Mogk, S., Wolburg, H., Frey, C., Kubata, B., and Duszenko, M. (2012). Brain infection by African trypanosomes during sleeping sickness. Neurol. Psychiatr. Brain Res. *18*, 49–51.

Mshelbwala, A.S. (1972). *Trypanosoma brucei* infection in the haemocoel of tsetse flies. Trans. R. Soc. Trop. Med. Hyg. *66*, 637–643. https://doi.org/10.1016/0035-9203(72)90310-0.

Myburgh, E., Coles, J.A., Ritchie, R., Kennedy, P.G., McLatchie, A.P., Rodgers, J., Taylor, M.C., Barrett, M.P., Brewer, J.M., and Mottram, J.C. (2013). *In vivo* imaging of trypanosome-brain interactions and development of a rapid screening test for drugs against CNS stage trypanosomiasis. PLoS Negl. Trop. Dis. *7*, e2384. https://doi.org/10.1371/journal.pntd.0002384.

Narita, K., and Takeda, S. (2015). Cilia in the choroid plexus: their roles in hydrocephalus and beyond. Front. Cell. Neurosci. *9*, 39. https://doi.org/10.3389/fncel.2015.00039.

Nikolskaia, O.V., de, A.L.A.P., Kim, Y.V., Lonsdale-Eccles, J.D., Fukuma, T., Scharfstein, J., and Grab, D.J. (2006). Blood-brain barrier traversal by African trypanosomes requires calcium signaling induced by parasite cysteine protease. J. Clin. Invest. *116*, 2739–2747. https://doi.org/10.1172/JCI27798.

Otieno, L.H., Darji, N., and Onyango, P. (1976). Development of Trypanosoma (Trypanozoon) brucei in Glossina morsitans inoculated into the tsetse haemocoel. Acta Trop. *33*, 143–150.

Pentreath, V.W., Owolabi, A.O., and Doua, F. (1992). Survival of *Trypanosoma brucei* brucei in cerebrospinal fluid. Ann. Trop. Med. Parasitol. *86*, 29–34.

Reddy, G.S., Mukhopadhyay, A.G., and Dey, C.S. (2017). Characterization of ciliobrevin A mediated dynein ATPase inhibition on flagellar motility of Leishmania donovani. Mol. Biochem.Parasitol. *214*, 75–81. https://doi.org/10.1016/j.molbiopara.2017.04.003.

Reuner, B., Vassella, E., Yutzy, B., and Boshart, M. (1997). Cell density triggers stumpy differentiation of *Trypanosoma brucei* bloodstream forms in culture. Mol. Biochem. Parasitol. *90*, 269–280.

<img referenced to be CellPress OPEN ACCESS> <img referenced to be iScience Article>

Rojas, F., Silvester, E., Young, J., Milne, R., Tettey, M., Houston, D.R., Walkinshaw, M.D., Perez-Pi, I., Auer, M., Denton, H., et al. (2019). Oligopeptide signaling through TbGPR89 drives trypanosome quorum sensing. Cell 176, 306–317.e16. https://doi.org/10.1016/j.cell.2018.10.041.

Ross, R., and Thomson, D. (1910). A case of sleeping sickness studied by precise enumerative methods: regular periodical increase of the parasites disclosed. Proc. R. Soc. B Biol. Sci. 82, 411–415.

Schmidt, H., and Bafort, J.M. (1985). African trypanosomiasis: treatment-induced invasion of brain and encephalitis. Am. J. Trop. Med. Hyg. 34, 64–68.

Schmidt, H., and Bafort, J.M. (1987). African trypanosomiasis: haematogenic brain parasitism early in experimental infection through bypassing the blood-brain barrier, with considerations on brain trypanosomiasis in man. Parasitol. Res. 73, 15–21.

Schultzberg, M., Ambatsis, M., Samuelsson, E., Kristensson, K., and Van Meirvenne, N. (1988). Spread of Trypanosoma brucei to the nervous system: early attack on circumventricular organs and sensory ganglia. J. Neurosci. Res. 21, 56–61.

Schwerk, C., Papandreou, T., Schuhmann, D., Nickol, L., Borkowski, J., Steinmann, U., Quednau, N., Stump, C., Weiss, C., Berger, J., et al. (2012). Polar invasion and translocation of Neisseria meningitidis and Streptococcus suis in a novel human model of the blood-cerebrospinal fluid barrier. PLoS One 7, e30069. https://doi.org/10.1371/journal.pone.0030069.

Seed, J.R., and Black, S.J. (1997). A proposed density-dependent model of long slender to short stumpy transformation in the African trypanosomes. J. Parasitol. 83, 656–662.

Shimogawa, M.M., Ray, S.S., Kisalu, N., Zhang, Y., Geng, Q., Ozcan, A., and Hill, K.L. (2018). Parasite motility is critical for virulence of African trypanosomes. Sci. Rep. 8, 9122. https://doi.org/10.1038/s41598-018-27228-0.

Srinivasan, B., Kolli, A.R., Esch, M.B., Abaci, H.E., Shuler, M.L., and Hickman, J.J. (2015). TEER measurement techniques for in vitro barrier model systems. J. Lab. Autom. 20, 107–126. https://doi.org/10.1177/2211068214561025.

Steinmann, U., Borkowski, J., Wolburg, H., Schroppel, B., Findeisen, P., Weiss, C., Ishikawa, H., Schwerk, C., Schroten, H., and Tenenbaum, T. (2013). Transmigration of polymorphnuclear neutrophils and monocytes through the human blood-cerebrospinal fluid barrier after bacterial infection in vitro. J. Neuroinflammation 10, 31. https://doi.org/10.1186/1742-2094-10-31.

Stevenson, B.R., and Begg, D.A. (1994). Concentration-dependent effects of cytochalasin D on tight junctions and actin filaments in MDCK epithelial cells. J. Cell Sci. 107, 367–375.

Sudarshi, D., Lawrence, S., Pickrell, W.O., Eligar, V., Walters, R., Quaderi, S., Walker, A., Capewell, P., Clucas, C., Vincent, A., et al. (2014). Human African trypanosomiasis presenting at least 29 years after infection–what can this teach us about the pathogenesis and control of this neglected tropical disease? PLoS Negl. Trop. Dis. 8, e3349. https://doi.org/10.1371/journal.pntd.0003349.

Sun, S.Y., Kaelber, J.T., Chen, M., Dong, X., Nematbakhsh, Y., Shi, J., Dougherty, M., Lim, C.T., Schmid, M.F., Chiu, W., and He, C.Y. (2018). Flagellum couples cell shape to motility in Trypanosoma brucei. Proc. Natl. Acad. Sci. U S A 115, E5916–E5925. https://doi.org/10.1073/pnas.1722618115.

Theile, M., Wiora, L., Russ, D., Reuter, J., Ishikawa, H., Schwerk, C., Schroten, H., and Mogk, S. (2019). A simple approach to perform TEER measurements using a self-made volt-amperemeter with programmable output frequency. J. Vis. Exp. https://doi.org/10.3791/60087.

Tietz, S., and Engelhardt, B. (2015). Brain barriers: crosstalk between complex tight junctions and adherens junctions. J. Cell Biol. 209, 493–506. https://doi.org/10.1083/jcb.201412147.

Trindade, S., Rijo-Ferreira, F., Carvalho, T., Pinto-Neves, D., Guegan, F., Aresta-Branco, F., Bento, F., Young, S.A., Pinto, A., Van Den Abbeele, J., et al. (2016). Trypanosoma brucei parasites occupy and functionally adapt to the adipose tissue in mice. Cell Host Microbe 19, 837–848. https://doi.org/10.1016/j.chom.2016.05.002.

Uppaluri, S., Nagler, J., Stellamanns, E., Heddergott, N., Herminghaus, S., Engstler, M., and Pfohl, T. (2011). Impact of microscopic motility on the swimming behavior of parasites: straighter trypanosomes are more directional. PLoS Comput. Biol. 7, e1002058. https://doi.org/10.1371/journal.pcbi.1002058.

Vandenhaute, E., Stump-Guthier, C., Lasierra Losada, M., Tenenbaum, T., Rudolph, H., Ishikawa, H., Schwerk, C., Schroten, H., Durken, M., Marz, M., and Karremann, M. (2015). The choroid plexus may be an underestimated site of tumor invasion to the brain: an in vitro study using neuroblastoma cell lines. Cancer Cell Int. 15, 102. https://doi.org/10.1186/s12935-015-0257-2.

Welburn, S.C., Molyneux, D.H., and Maudlin, I. (2016). Beyond tsetse–implications for research and control of human african trypanosomiasis epidemics. Trends Parasitol. 32, 230–241. https://doi.org/10.1016/j.pt.2015.11.008.

Wolburg, H., Mogk, S., Acker, S., Frey, C., Meinert, M., Schonfeld, C., Lazarus, M., Urade, Y., Kubata, B.K., and Duszenko, M. (2012). Late stage infection in sleeping sickness. PLoS One 7, e34304. https://doi.org/10.1371/journal.pone.0034304.

Wurapa, F.K., Dukes, P., Njelesani, E.K., and Boatin, B. (1984). A "healthy carrier" of Trypanosoma rhodesiense: a case report. Trans. R. Soc. Trop. Med. Hyg. 78, 349–350.

STAR★METHODS

KEY RESOURCES TABLE

REAGENT or RESOURCE	SOURCE	IDENTIFIER
Chemicals, peptides, and recombinant proteins		
IMDM	Sigma	I7633
Sodium hydrogen carbonate	Sigma	#1063232500
Hypoxanthine	Sigma	H9636
L-Cysteine	Sigma	C7352
Pyruvate	Sigma	P5280
Thymidine	Sigma	T1895
BCS	Carl Roth	KK28.1
Mercaptoethanol	Sigma	M3148
Pen/Strep	Sigma	P4333
FBS	LifeTechnologies	#10270106
Serum Plus TM	Sigma	14009C
G418	Sigma	A1720
Hygromycin	Sigma	H3274
Puromycin	Sigma	P8833
Phleomycin	Sigma	P9564
DMEM:F12	Gibco	#31330-038
FBS	LifeTechnologies	#10270106
Pen/Strep	Sigma	P4333
Insulin	Sigma	#I9278
Experimental models:Cell lines		
MiTat 1.2 VSG 221	this paper	none
MiTat 1.2 SMB-p2T7-MSP-B	this paper	none
AnTat 1.1E	this paper	none
GVR35-mCherry	(Myburgh et al., 2013)	none
MiTat 1.2 PC117	this paper	none
MiTat 1.2 PC1313-514-α-Tub	this paper	none
HIBCPP cells	(Schwerk et al., 2012)	none
Critical commercial assays		
Filter inserts 3μm/8μm	Greiner Bio-One	#662631/#662638
Dextran blue 5kDa	Sigma	90008-1G
Cytochalasin D	Sigma	C8273-1MG
Ciliobrevin A	Sigma	H4541-5MG
QIAamp DNA Mini Kit	Qiagen	#51304
Fast SYBR Green MasterMix	Applied Biosystems	# 4385610
Rneasy Mini Kit	Qiagen	#74104
Power SYBR Green RNA-to-CT™ 1-Step Kit	Applied Biosystems	# 4391178
rabbit anti-Tb VSG221	this paper	none
donkey anti-rabbit AF 594	antibodies-online	ABIN2667002
Phalloidin-Alexa Fluor 488	Invitrogen	A12379
Bisbenzimide	Sigma	#14533
Cellmask Green PM stain	Thermo Fisher	C37608

(Continued on next page)

Continued		
REAGENT or RESOURCE	SOURCE	IDENTIFIER
Oligonucleotides		
5'-AAACGGCCTCGTTGATACAC-3'	Invitrogen	TbAOX fwd
5'-TGCTGAGGTTCCAGTACACG-3'	Invitrogen	TbAOX rev
5'-GTGGCTGGCGTAACTAACCT-3'	Invitrogen	TbMSP-B fwd
5'-TGTGATAATGCGGTGCCACT-3'	Invitrogen	TbMSP-B rev
5'-CTCCTCCTCGTCGAACTCGCCCT-3'	Invitrogen	Tubulin fwd
5'-ATGCGCGAAATCGTCTGCGTTCAG-3'	Invitrogen	Tubulin rev
5'-CACAGCCACACAAAAGACCG-3'	Invitrogen	GAPDH fwd
5'-CGCGTCGCAATGAAGGTAAG-3'	Invitrogen	GAPDH rev

RESOURCE AVAILABILITY

Lead contact

Requests for further information should be directed to the lead contact (Stefan Mogk, stefan.mogk@uni-tuebingen.de).

Materials availability

General materials and reagents used in this study are commercially available with no restrictions. Trypanosome strains are available from the lead contact. HIBCPP cells are available from C.S. and H.S. with a completed Material Transfer Agreement.

Data and code availability

- All data reported in this paper will be shared by the lead contact upon request.

- This paper does not report original code.

- Any additional information required to reanalyze the data reported in this paper is available from the lead contact upon request.

EXPERIMENTAL MODEL AND SUBJECT DETAILS

Trypanosoma brucei brucei strains

Bloodstream form parasites (Table) were cultured in HMI-9 at 37°C. Monomorphic bloodstream form parasites: MiTat 1.2 VSG 221, MiTat 1.2 SMB-p2T7-MSP-B (T7RNAP TETR NEO RDNA::T7PRO^Ti MSP-B HYG; selected with 2 μg/ml G418, 2.5 μg/ml hygromycin). Pleomorphic bloodstream form parasites: AnTat 1.1E (kindly provided by Markus Engstler, University of Würzburg), GVR35-mCherry (MCHERRY PURO; 0.5 μg/ml puromycin; kindly provided by Jeremy Mottram, University of York). Procyclic parasites (Table 1) were cultured in PC medium at 28°C: MiTat 1.2 PC117, MiTat 1.2 PC1313-514-alpha-Tubulin (TETR BLE T7RNAP NEO RDNA::T7PRO^Ti ATUB HYG, selected with 5 μg/ml phleomycin, 50 μg/ml G418, 15 μg/ml hygromycin). In some experiments, procyclic cells were incubated in trypanosome dilution buffer (PBS with 20 mM glucose) containing 500 μM ciliobrevin A (in DMSO). For transmigration experiments of fixed trypanosomes MiTat 1.2 VSG 221 cells were incubated in 0.25% formaldehyde (10 min) and subsequently washed with TDB before applying to respective HIBCPP filters.

METHOD DETAILS

In vitro BCB

Human choroid plexus papilloma cells (HIBCPP) were harvested from culture flasks by trypsinization and centrifugation (50 g, 10 min). 1e5 cells were seeded on a cell culture filter insert (Greiner, ThinCert 3 μm translucent PET cell culture inserts, 33 mm^2) in DMEM:F12 (containing 10% fetal calf serum and 5 μg/ml insulin); for details see (Dinner et al., 2016). TEER was measured daily with a self-made voltammeter (Theile et al., 2019). Medium was changed every second day until the filters reached an impedance of 300 Ω (100 Ω cm^2). Then, medium was changed to serum-free DMEM:F12, since cultivation in serum-free medium causes formation of a higher TEER by choroid plexus epithelial cells *in vitro* (Haselbach et al., 2001;

Schwerk et al., 2012). Once the filter reached an impedance of 600 Ω (200 Ω cm^2) it was used for experiments. To measure barrier permeability, 75 μL dextran blue (5 kDa, stock solution of 133 mg/ml in DPBS) were added together with 375 μL DMEM:F12 to the upper compartment and incubated for 2 h at 37°C. Extinction of the medium in the lower compartment was measured at 595 nm against DMEM:F12 medium without dextran blue using a 96 well Dynex MRX plate reader. In some experiments, cytochalasin D was added to a final concentration of 1 μg/ml for 2 hours to disturb tight junction formation (Dinner et al., 2016). If not differently stated, filters for transmigration experiments were transferred to wells containing 1 ml HMI-9 medium and 5e6 trypanosomes were added (in 500 μl HMI-9) to the upper compartment. After 2 h (or the specified period), DNA of transmigrated trypanosomes was isolated and quantified. For ciliobrevin A experiments, procyclic cells were preincubated for 15 min in PBS/ 20mM glucose/ 500μM ciliobrevin A and transferred to the upper reservoir of a Transwell filter insert (3 μm pore size) without HIBCPP cells (which do not tolerate ciliobrevin).

DNA/RNA purification

500 μl of the lower reservoir were directly mixed with proteinase K. Total DNA was purified as described in the QIAamp DNA Mini instruction manual (section "Blood and Body Fluids") and stored at -20°C for further analysis. As qPCR standard, DNA purification was carried out with a defined number of trypanosomes (1e3, 1e4, 1e5 or 1e6 trypanosomes/500 μl). RNA was isolated from 1e7 cells with a QIAGEN Rneasy kit, DNA contamination was digested with Dnase I.

Quantitative PCR

DNA templates were mixed with Fast SYBR Green Master Mix (Applied Biosystems), TbAOX primers (10 μM final concentration, fwd: 5′-AAACGGCCTCGTTGATACAC-3′, rev: 5′-TGCTGAGGTTCCAGTACACG-3′) and nuclease-free water in a 96-well PCR plate. qPCR was carried out using the QuantStudio PCR cycler together with the QuantStudio Design and Analysis software. Quantitative reverse-transcriptase PCR was done with Power SYBR Green RNA-to-Ct™ (Applied Biosystems) and primers against TbMSP-B (fwd: 5′-GTGGCTGGCGTAACTAACCT-3′, rev: 5′-TGTGATAATGCGGTGCCACT-3′), tubulin (fwd: 5′-CTCCTCC TCGTCGAACTCGCCCT-3′, rev: 5′-ATGCGCGAAATCGTCTGCGTTCAG-3′) or GAPDH (fwd: 5′-CACAGC CACACAAAAGACCG-3′, rev: 5′-CGCGTCGCAATGAAGGTAAG-3′).

Measurement of trypanosome motility

Trypanosomes were filmed with 344x258 pixels and 10 frames/s (microscope BH2 RFCA with camera F-view II, Olympus® Soft Imaging System GmbH). With GIMP version 2.8.0, the position of the posterior end was marked in 30 frames and plotted to a path in one combined layer.

Imaging of HIBCPP filter membranes

For immunostaining, filters were fixed for 10 min at room temperature in 3.7% (w/v) paraformaldehyde, washed 5 min with PBS, permeabilized 5 min in 0.1% (v/v) triton/PBS and blocked 20 min in 1% (w/v) BSA/PBS. Rabbit anti-221 (1:1000) was applied in 1% (w/v) BSA/PBS for 1 h. Filters were washed three times for 5 min. Filters were incubated 30 min with anti-rb-AF594 (1:500), phalloidin-AF 488 (1:250) and bisbenzimide (1 g/ml) and washed 5 times in 1% (w/v) BSA/PBS. Images were acquired with Zeiss Axio Observer.Z1 Apotome and Axiovision software using Plan-Apochromat 63x/1.40 Oil M27 objective lens. The image acquisition was carried out using the Zeiss scanning software Axiovision 4.6. For surface electron microscopy, samples were fixed with 2.5% (v/v) glutaraldehyde in cacodylate buffer, postfixed with 1% osmium tetroxide in phosphate-buffered saline, dehydrated in a graded series of ethanol and critical-point-dried using CO2. Afterwards cells were fixed on specimen holder stubs, sputter-coated with gold, and viewed with a scanning electron microscope (SEM) (Cambridge Stereoscan 250 Mk2, Cambridge Scientific, Cambridge, UK) (Mogk et al., 2014b). For live-cell imaging, fluorescent (mCherry) GVR35 trypanosomes were used. HIBCPP cells were stained for 10 minutes with ThermoFisher CellMask™ Green Plasma Membrane Stain (1:1000). Videos were recorded with Zeiss Axio Observer.Z1/7 (objective LD Plan-Neofluar 40x/0.6 Korr Ph 2 M27) as timelapse with 0.5 images per second.

Abbreviations

AAA+: ATPase associated with various cellular activities, AnTat: Antwerp Trypanozoon antigen type, AOX: alternative oxidase, BBB: blood-brain barrier, BCB: blood-cerebrospinal fluid barrier, BSA: bovine serum albumin, CSF: cerebrospinal fluid, DMEM:F12: Dulbecco's Modified Eagle Medium/Nutrient Mixture

F-12, FITC: fluorescein isothiocyanate, GAPDH: glyceraldehyde-3-phosphate dehydrogenase, HAT: Human African Trypanosomiasis, HIBCPP: Human choroid plexus papilloma cells, HMI: Hirumi's modified Iscove's medium, IC: inverse culture, MiTat: Molteno Institute Trypanozoon antigenic type, MSP-B: major surface metalloprotease B, NC: normal culture, PET: polyethylene terephthalate, qPCR: quantitative polymerase chain reaction, SIF: stumpy induction factor, SMB: single marker bloodstream form, TEER: transepithelial electrical resistance, VSG: variant surface glycoprotein.

Ethics statement

HIBCPP cells have been obtained from Prof. Ishikawa (Department of NDU Life Sciences, School of Life Dentistry at Tokyo, The Nippon Dental University). The ethical committee of the Nippon Dental University has confirmed in 2000 that no ethical approval is necessary since no connection from the donor patient to the cells could be made. This study was carried out in strict accordance with the German Animal Welfare Act. The Regional Commission of Tuebingen had approved propagation of trypanosomes in Wistar rats (permit number: IB 3/10).

QUANTIFICATION AND STATISTICAL ANALYSIS

Statistical analysis

For graphical presentations and statistical calculations, quantitative parameters are given by mean values and standard deviations. A 1-way ANOVA has been performed in order to test the influence of different trypanosome populations on transmigration efficiency. A test result with $p < 0.05$ has been considered as statistically significant.